

**NUMERICAL STUDY ON FREE CONVECTION FLOW WITH JOULE HEATING,  
HEAT GENERATION AND VISCOUS DISSIPATION ALONG A VERTICAL  
WAVY SURFACE**

A dissertation submitted to the  
Department of Mathematics  
Bangladesh University of Engineering and Technology  
In fulfilment of the requirement for the award of the degree of

**Masters of Science  
in  
Mathematics**

**Submitted by**  
**Md. Nurul Amin**  
Student No. 1015092506  
Session: October-2015



Department of Mathematics  
Bangladesh University of Engineering & Technology  
Dhaka- 1000, Bangladesh  
14<sup>th</sup> July 2018

The dissertation titled  
**NUMERICAL STUDY ON FREE CONVECTION FLOW WITH JOULE HEATING,  
HEAT GENERATION AND VISCOUS DISSIPATION ALONG A VERTICAL  
WAVY SURFACE**

**Submitted by  
Md. Nurul Amin**

Student No. 1015092506, Session: October 2015, a student of M. Sc has been accepted as  
satisfactory in fulfilment of the requirement of the degree of

**Masters of Science in Mathematics**

On July 2018

**Board of Examiners**

- N. Parveen*  
.....
- (i) Name: Dr. Nazma Parveen  
Address: Professor  
Department of Mathematics  
BUET, Dhaka-1000  
Chairman  
(Supervisor)
- N. Rahman*  
.....
- (ii) Name: Head  
Address: Department of Mathematics  
BUET, Dhaka-1000  
Member  
(Ex-Officio)
- A. Alim*  
.....
- (iii) Name: Dr. Md. Abdul Alim  
Address: Professor  
Department of Mathematics  
BUET, Dhaka-1000  
Member
- S. Parvin*  
.....
- (iv) Name: Dr. Salma Parvin  
Address: Professor  
Department of Mathematics  
BUET, Dhaka-1000  
Member
- M. Kamal Chowdhury*  
.....
- (v) Name: Dr. Md. Mustafa Kamal Chowdhury  
Address: Ex-Professor  
110 Lake Garden  
Lake Circus Lane-3  
Dhaka-1205  
Member  
(External)

## **DEDICATIONS**

This work is dedicated to my beloved

**Family**  
&  
**Teacher (Professor Dr. Nazma Parveen)**

## **Author's Declaration**

I hereby declare that the work which is being presented in this dissertation entitled **“NUMERICAL STUDY ON FREE CONVECTION FLOW WITH JOULE HEATING, HEAT GENERATION AND VISCOUS DISSIPATION ALONG A VERTICAL WAVY SURFACE”** was being carried out in accordance with the regulations of Bangladesh University of Engineering & Technology (BUET), Dhaka, Bangladesh. This is an authentic record of my own work.

This dissertation has not been submitted elsewhere (university or institution) for the award of any other degree in home or abroad.

*Md. Nurul Amin*  
14/07/2018  
(Md. Nurul Amin)

## Acknowledgement

At first all praise belongs to *Almighty Allah*

I would like to express my earnest gratitude, intense thankfulness and indebtedness to my esteemed supervisor Dr. Nazma Parveen, Professor, Department of Mathematics, Bangladesh University of Engineering and Technology (BUET), Dhaka- 1000 under whose careful supervision and guidance, I have been able to accomplish this dissertation.

I also express my gratitude to all my respectable teachers, Department of Mathematics, BUET especially to professor Dr. Md. Mustafizur Rahman, Dr. Md. Mustafa Kamal Chowdhury, Dr. Md. Abdul Alim and Dr. Salma Parvin, for their kind help and heartiest co-operation. It is my first thesis and I want to give special thanks to Dr. Md. Mustafa Kamal Chowdhury and Dr. Salma Parvin . Without their cordial co-operation in finding any kind of mistakes it would be very difficult for me to write a successful thesis paper.

Finally, I must acknowledge my debt to my parents for whom I have been able to see the beautiful sights and sounds of the world. Last but not the least, it would be ungrateful for me if I do not evaluate the efforts and pains of my sister and brother.

Md. Nurul Amin

14<sup>th</sup> July 2018



## Abstract

A steady two-dimensional natural convection flow of viscous incompressible fluid considering viscous dissipation along a uniformly heated vertical wavy surface in presence of internal heat generation and Joule heating has been investigated. Using the appropriate transformations the basic equations are changed to non-dimensional boundary layer equations, which are solved numerically by employing the implicit finite difference method together with Keller-box scheme. The program code of this method has been developed in FORTRAN.

Here I have focused my attention on the changes of surface shear stress in terms of local skin friction, rate of heat transfer in terms of local Nusselt Number, velocity profile, temperature distribution, isotherms as well as the streamlines for a selection of parameter sets consisting of heat generation parameter  $Q$ (0.30 to 1.0) the Joule heating parameter  $J$ (0.001 to 0.040), the magnetic parameter  $M$ (0.0 to 3.0), viscous dissipation parameter  $Ec$ (0.50 to 5.0), Prandtl number  $Pr$ (0.73 to 7.00) and the amplitude of waviness of the surface  $\alpha$ (0.0 to 0.3). The results have been shown graphically by utilizing the visualizing software TECHPLOT. The results obtained from the numerical study have been discussed emphasizing the physical prospects.

## Nomenclature

- $C_p$  : Specific heat at constant pressure
- $C_{fx}$  : Local skin friction coefficient
- $N_{ux}$  : Local Nusselt number
- $Gr$  : Grashof number
- $f$  : Dimensionless stream function
- $g$  : Acceleration due to gravity
- $h$  : Heat flux coefficient
- $q_w$  : Heat flux at the surface
- $L$  : Wave length associated with wavy surface
- $k$  : Thermal conductivity
- $J$  : Joule heating parameter
- $Q$  : Heat generation parameter
- $Q_0$  : Heat generation constant
- $Pr$  : Prandtl number
- $\bar{p}$  : Pressure of the fluid
- $p$  : Dimensionless pressure function
- $T$  : Fluid temperature in the boundary layer
- $T_\infty$  : Temperature of the ambient fluid
- $T_w$  : Temperature at the surface
- $(U, V)$  : Velocity component along x and y
- $(u, v)$  : Dimensionless velocity component
- $(X, Y)$  : Axis in the direction along and normal to the tangent of the surface
- $(x, y)$  : Non-dimensional coordinate system
- $\Delta\psi$  : Distance between two streamlines
- $\Delta\theta$  : Distance between two isotherms
- $n$  : Wave number indicator

## Greek Symbols

- $\alpha$  : Amplitude of the wavy surface
- $\beta$  : Volumetric coefficient of thermal expansion
- $\nu$  : Kinematic viscosity
- $\psi$  : Stream function
- $\eta$  : Dimensionless similarity variable
- $\tau_w$  : Shearing stress
- $\mu$  : Dynamic viscosity
- $\rho$  : Density of the fluid
- $\theta$  : Dimensionless temperature function
- $\sigma_0$  : Electrical conductivity of the fluid
- $\beta_0$  : Applied magnetic field
- $\sigma_x$  : Non-dimensional surface profile function
- $\overline{\sigma}$  : Surface profile function

## Subscripts

- $W$  : Wall conditions
- $\infty$  : Ambient Condition

## Superscripts

- $'$  : Differentiation with respect to  $\eta$
- $-$  : Dimensional quantity



<b>Contents</b>	<b>Pages</b>
<b>Chapter One</b>	
<b><i>Introduction</i></b>	<b>01-04</b>
1.1 Literature Review	05-06
1.2 Main Objectives of present works	07
1.3 Outline of Methodology	08
<b>Chapter Two</b>	
<b><i>Mathematical modeling of the flow problem</i></b>	<b>09</b>
2.1 Governing equations of the flow	09-14
2.2 Transformation of the governing equations	15-17
2.3 Implicit Finite Difference Method (IFDM)	17-22
<b>Chapter Three</b>	
<b><i>Effects of Joule Heating, Heat generation and Viscous Dissipation on Free Convection Flow along a Vertical Wavy Surface</i></b>	<b>23-54</b>
3.1 Introduction	23
3.2 Results and discussion	24-55
3.3 Conclusion of this Chapter	56
<b>Conclusion</b>	<b>57-58</b>
<b>Extension of this work</b>	<b>59</b>
<b>References</b>	<b>60-61</b>

## List of Figures

- Fig 2.1** The coordinate system and the physical model
- Fig 2.2** Net rectangle of difference approximations for the box scheme
- Fig 3.1** Velocity and temperature profiles for different values of heat generation parameter  $Q$  while  $Pr = 0.73$ ,  $\alpha = 0.2$ ,  $J=0.01$ ,  $Ec = 0.02$ ,  $M = 0.5$
- Fig 3.2** Velocity and temperature profiles for different values of  $J$  while  $Pr = 0.73$ ,  $\alpha = 0.2$ ,  $Ec = 0.02$ ,  $M = 0.01$   $Q = 0.3$
- Fig 3.3** Velocity and temperature profiles for different values of  $M$  while  $Pr = 0.73$ ,  $\alpha = 0.2$ ,  $Ec = 0.02$ ,  $J = 0.01$   $Q = 0.3$
- Fig 3.4** Velocity and temperature profiles for different values of Viscous dissipation parameter  $Ec$  while  $Pr = 0.73$ ,  $\alpha = 0.2$ ,  $J = 0.01$ ,  $M = 0.02$ ,  $Q = 0.30$
- Fig 3.5** Velocity and temperature profiles for different values of  $Pr$  while  $J = 0.04$ ,  $\alpha = 0.2$ ,  $Ec = 0.02$ ,  $Q = 0.3$ ,  $M = 0.01$
- Fig 3.6** Velocity and temperature profiles for different values of  $\alpha$  while  $Pr = 0.73$ ,  $Q = 0.3$ ,  $J = 0.04$ ,  $Ec = 0.02$ ,  $M = 0.01$
- Fig 3.7** Skin friction coefficient ( $C_{fx}$ ) and rate of heat transfer ( $Nux$ ) for different values of heat generation parameter  $Q$  while  $Pr = 0.73$ ,  $\alpha = 0.2$ ,  $J = 0.01$ ,  $Ec = 0.02$ ,  $M = 0.50$
- Fig 3.8** Skin friction coefficient ( $C_{fx}$ ) and rate of heat transfer ( $Nux$ ) for different values of  $J$  while  $Pr = 0.73$ ,  $\alpha = 0.2$ ,  $Ec = 0.02$ ,  $M = 0.01$   $Q = 0.3$
- Fig 3.9** Skin friction coefficient ( $C_{fx}$ ) and rate of heat transfer ( $N_{ux}$ ) for different values of Magnetic parameter  $M$  while  $Pr = 0.73$ ,  $\alpha = 0.2$ ,  $J = 0.01$ ,  $Ec = 0.02$ ,  $Q = 0.30$
- Fig 3.10** Skin friction coefficient ( $C_{fx}$ ) and rate of heat transfer ( $Nux$ ) for different values of  $Ec$  while  $Pr = 0.73$ ,  $\alpha = 0.2$ ,  $J = 0.01$ ,  $Q = 0.3$ ,  $M = 0.02$
- Fig 3.11** Skin friction coefficient ( $C_{fx}$ ) and rate of heat transfer ( $Nux$ ) for different values of heat generation parameter  $Pr$  while  $Q = 0.30$ ,  $\alpha = 0.20$ ,  $J = 0.04$ ,  $Ec = 0.02$ ,  $M = 0.01$
- Fig 3.12** Skin friction coefficient ( $C_{fx}$ ) and rate of heat transfer ( $Nux$ ) for different values of  $\alpha$  while  $Pr = 0.73$ ,  $Q = 0.3$ ,  $J = 0.04$ ,  $Ec = 0.02$ ,  $M = 0.01$
- Fig 3.13** Streamlines for (a)  $Q = 0.30$ , (b)  $Q = 0.50$ , (c)  $Q = 0.70$  and (d)  $Q = 1.0$  while  $Pr = 0.73$ ,  $\alpha = 0.3$ ,  $J = 0.01$ ,  $Ec = 0.02$ ,  $M = 0.5$



- Fig 3.14** Isotherms for (a)  $Q = 0.30$ , (b)  $Q = 0.50$ , (c)  $Q = 0.70$  and (d)  $Q = 1.0$  while  $Pr = 0.73$ ,  $\alpha = 0.3$ ,  $J = 0.01$ ,  $Ec = 0.02$ ,  $M = 0.5$
- Fig 3.15** Streamlines for (a)  $J = 0.001$ , (b)  $J = 0.009$ , (c)  $J = 0.020$  and (d)  $J = 0.040$  while  $Pr = 0.73$ ,  $\alpha = 0.2$ ,  $M = 0.01$ ,  $Ec = 0.02$
- Fig 3.16** Isotherms for (a)  $J = 0.001$ , (b)  $J = 0.009$ , (c)  $J = 0.020$  and (d)  $J = 0.040$  while  $Pr = 0.73$ ,  $\alpha = 0.2$ ,  $M = 0.01$ ,  $Ec = 0.02$
- Fig 3.17** Streamlines for (a)  $M = 0.0$ , (b)  $M = 1.0$ , (c)  $M = 2.0$  and (d)  $M = 3.0$  while  $Pr = 0.73$ ,  $\alpha = 0.2$ ,  $Ec = 0.02$ ,  $Q = 0.3$
- Fig 3.18** Isotherms for (a)  $M = 0.0$ , (b)  $M = 1.0$ , (c)  $M = 2.0$  and (d)  $M = 3.0$  while  $Pr = 0.73$ ,  $\alpha = 0.2$ ,  $Ec = 0.02$ ,  $Q = 0$ .
- Fig 3.19** Streamlines for (a)  $Ec = 0.50$ , (b)  $Ec = 2.00$ , (c)  $Ec = 3.50$  and (d)  $Ec = 5.00$  while  $Pr = 0.73$ ,  $\alpha = 0.2$ ,  $J = 0.01$ ,  $M = 0.02$
- Fig 3.20** Isotherms for (a)  $Ec = 0.50$ , (b)  $Ec = 2.00$ , (c)  $Ec = 3.50$  and (d)  $Ec = 5.00$  while  $Pr = 0.73$ ,  $\alpha = 0.2$ ,  $J = 0.01$ ,  $Q = 0.3$ ,  $M = 0.02$
- Fig 3.20** Isotherms for (a)  $Ec = 0.50$ , (b)  $Ec = 2.00$ , (c)  $Ec = 3.50$  and (d)  $Ec = 5.00$  while  $Pr = 0.73$ ,  $\alpha = 0.2$ ,  $J = 0.01$ ,  $Q = 0.3$ ,  $M = 0.02$
- Fig 3.21** Streamlines for (a)  $Pr = 0.73$ , (b)  $Pr = 1.74$ , (c)  $Pr = 3.00$  and (d)  $Pr = 7.00$  while  $Q = 0.30$ ,  $\alpha = 0.2$ ,  $J = 0.04$ ,  $Ec = 0.02$ ,  $M = 0.01$
- Fig 3.22** Isotherms for (a)  $Pr = 0.73$ , (b)  $Pr = 1.74$ , (c)  $Pr = 3.00$  and (d)  $Pr = 7.00$  while  $Q = 0.30$ ,  $\alpha = 0.2$ ,  $J = 0.04$ ,  $Ec = 0.02$ ,  $M = 0.01$
- Fig 3.23** Streamlines for (a)  $\alpha = 0.0$ , (b)  $\alpha = 0.1$ , (c)  $\alpha = 0.2$  and (d)  $\alpha = 0.3$  while  $Pr = 0.73$ ,  $Q = 0.3$ ,  $J = 0.04$ ,  $Ec = 0.02$ ,  $M = 0.01$
- Fig 3.24** Isotherms for (a)  $\alpha = 0.0$ , (b)  $\alpha = 0.1$ , (c)  $\alpha = 0.2$  and (d)  $\alpha = 0.3$  while  $Pr = 0.73$ ,  $Q = 0.3$ ,  $J = 0.04$ ,  $Ec = 0.02$ ,  $M = 0.01$

## List of Tables

- Table 3.1** Skin friction coefficient and rate of heat transfer for the different values of Joule Heating parameter ( $J$ )
- Table 3.2** Comparison and code validations

# Chapter One

## Introduction

---

Natural Convection is a type of heat transfer which occurs only due to density differences in the fluid due to temperature gradients. In natural convection, fluid surrounding a heat source receives heat, becomes less dense and rises up. The surrounding fluid then moves to replace it. This cooler fluid is then heated and the process continues, forming convection current. Since there is no external force to accelerate the heat transfer, the design of the heat sink should be thermally efficient to dissipate maximum amount of heat. The driving force for natural convection is buoyancy, a result of differences in fluid density. Because of this, the presence of a proper acceleration such as arises from resistance to gravity, or an equivalent force (arising from acceleration, centrifugal force or Coriolis effect), is essential for natural convection. For example, natural convection essentially does not operate in free-fall (inertial) environments, such as that of the orbiting International Space Station, where other heat transfer mechanisms are required to prevent electronic components from overheating. The natural convection procedures are governed essentially by three features namely the body force, the temperature difference in the flow field and the fluid density variations with temperature. The manipulation of natural convection heat transfer can be deserted in the case of large Reynolds number and very small Grashof number. Alternately, the natural convection should be the governing aspect for large Grashof number and small Reynolds number. The analysis of natural convection has become considerable interest to engineers and scientists since it is important in many industrial and natural problems. There are many physical processes in which buoyancy forces resulting from thermal diffusion play an important role in the convection transfer of heat. Few examples of the heat transfer by natural convection can be found in geophysics and energy related engineering problems such as natural circulation in geothermal reservoirs, refrigerator coils, hot radiator used for heating a room, transmission line, porous insulations, solar power collectors, spreading of pollutants etc. Natural convection flow is often encountered in cooling of nuclear reactors or in the study of the structure of stars and planets. In nature, convection cells formed from air raising

above sunlight-warmed land or water are a major feature of all weather systems. Convection is also seen in the rising plume of hot air from fire, oceanic currents, and sea-wind formation (where upward convection is also modified by Coriolis forces). In engineering applications, convection is commonly visualized in the formation of microstructures during the cooling of molten metals, and fluid flows around shrouded heat-dissipation fins, and solar ponds. A very common industrial application of natural convection is free air cooling without the aid of fans: this can happen on small scales (computer chips) to large scale process equipment

It is also necessary to study the heat transfer from an irregular surface because irregular surfaces often occur in many applications. It is often encountered in heat transfer devices to enhance heat transfer. Laminar natural convection flow from irregular surfaces can be used for transferring heat in several heat transfer devices, for examples, flat- plate solar collectors, flat-plat condensers in refrigerators, heat exchanger, functional clothing design, geothermal reservoirs and other industrial applications. They are widely used in space heating, refrigeration, air conditioning, power plants, chemical plants, petrochemical plants, petroleum refineries and natural gas processing. One common example of a heat exchanger is the radiator used in vehicles, in which the heat generated from engine transferred to air flowing through the radiator. Heat exchanger also widely used in industry both for cooling and heating large scale industrial process.

It is a model problem for the investigation of heat transfer from roughened surfaces in order to understand heat transfer enhancement. The sinusoidal wavy surface can be viewed as an approximation too much practical geometries in heat transfer. A good example is a cooling fin. Since cooling fins have a larger area than a flat surface, they are better heat transfer devices. Another example is a machine-roughened surface for heat transfer enhancement. The interface between concurrent or countercurrent two-phase flow is another example remotely related to this problem. Such an interface is always wavy and momentum transfer across it is by no means similar to that across a smooth, flat surface, and neither is the heat transfer. Also a wavy interface can have an important effect on the condensation process

Joule heating occurs when an electrical current is passed through a material and the material's resistivity to the current cause heat generation. Joule heating effects are common in electronic devices where the heat generated by a current may be an important influence.

For example, the ability to predict how electrical current will affect temperature distribution is useful when analyzing spot welding, circuit breakers, MEMS or electronic devices. Joule heating effects can be simulated by linking the results of electrostatic analysis to a steady-state or transient heat transfer analysis.

In electronic and in physics more broadly, Joule heating or ohmic heating refers to the increase in temperature of a conductor as a result of resistance to and electrical current flowing through it. At an atomic level, Joule heating is the result of moving electrons colliding with atoms in a conductor, whereupon momentum is transferred to the atom increasing its kinetic energy. When similar collisions cause a permanent structural change, rather than an elastic response, the result is known as eletro migration. Joule heating effect finds its application in electric heating devices such as electric heater, electric iron, bread toaster, even electric kettle and hair dryer etc

The presence of magnetic field in the effects of Joule heating is a very common phenomenon. A very common term Magnetohydrodynamic (MHD) is used to express magnetic field in the presence of electricity. Magnetohydrodynamic involves magnetic fields (magneto) and fluids (hydro) that conduct electricity and interact (dynamics). Magnetohydrodynamic (MHD) is the branch of continuum mechanics, which deals with the flow of electrically conducting fluids in electric and magnetic fields. MHD technology is based on a fundamental law of electromagnetism. Motion of the conducting fluid across the magnetic field induced electric currents which change the magnetic field and the action of the magnetic field on these currents give rise to mechanical forces, which modify the fluid. The interaction of the magnetic field and the moving electric charge carried by the flowing fluid induces a force, which tends to oppose the fluid motion and near the leading edge, the velocity is very small, so that the magnetic force that is proportional to the magnitude of the longitudinal velocity and acts in the opposite direction is also very small. Consequently, the influence of the magnetic field on the boundary layer is exerted only through induced forces within the boundary layer itself without additional effects arising from the free steam pressure gradient. Thus there is a two way interaction between the flow field and the magnetic field, the magnetic field exerts force on the fluid by producing induced currents and induced currents change the original magnetic field.

Many natural phenomena and engineering problems are susceptible to MHD analysis. It is useful in astrophysics. Geophysical encounter MHD phenomena in the interactions of the conducting fluids and magnetic fields those are present in and around heavenly bodies. Engineers employ MHD principles in the design of heat exchanger, pumps and flow meters, in space vehicles propulsion, control and re-entry, in creating novel power generating systems and developing confinement schemes for controlled fusion. The most important application of MHD are in the generation of electrical power with the electrically conducting fluid through a transverse magnetic field, electromagnetic pump, the MHD generator using ionized gas as an armature, electromagnetic pumping of liquid metal coolants in nuclear reactors. Other potential applications for MHD include electromagnets with fluid conductors, various energy conversion or storage devices and magnetically controlled lubrication by conducting fluids etc.

The viscous dissipation effect plays an important role in natural convection in various devices which are subjected to large deceleration or which operate at high rotational speeds and also in strong gravitational field processes on large scales (on large planets), in geological process and in nuclear engineering in connection with the cooling of reactors. The irreversible process by means of which the work done by a fluid on adjacent layers due to the action of shear forces transformed into heat is defined as viscous dissipation. It is also important in the flow of fluids having high viscosities. Temperature of the fluid increases because of it.

The study of temperature and heat transfer is of great importance to the engineers because of its almost universal occurrence in many branches of science and engineering. Heat generation is a volumetric phenomenon. That is, it occurs throughout the body of a medium. Therefore, the rate of heat generation in a medium is usually specified per unit volume. Heat generation is the ability to emit greater-than-normal heat from the body. The amount of heat generated or absorbed per unit volume is defined as  $Q(T - T_\infty)$ , where  $Q$  being a constant, which may take either positive or negative. The source term represents the heat generation when  $Q > 0$  and the heat absorption when  $Q < 0$ .

## 1.1 Literature Review

The laminar natural convection of a Newtonian fluid and heat transfer problem has been presented by many investigators because of its considerable practical applications. The effect of viscous dissipation in natural convection flow was investigated by Gebhart (1962). Further, he studied viscous dissipation effects in external natural convection flows with Mollendorf (1969). Keller (1978) carried out investigation on numerical methods in boundary layer theory. Yao (1983) analyzed natural convection along a vertical wavy surface. One year later I have found the investigation results for Physical and computational aspects of convective heat transfer by Cebeci and Bradshaw (1984). Moulic and Yao (1989) added uniform heat flux parameter on natural convection along a vertical wavy surface. Bhaynani and Bergles (1991) introduced sinusoidal wavy surface in natural convection heat transfer. Vejravelu and Hadjinicolaou (1993) investigated heat transfer in a viscous fluid over a stretching sheet with viscous dissipation and internal heat generation. Natural convection along a wavy vertical plate to non-newtonian fluids was studied by Kim (1997). In the same year Hossain and Rees analyzed on Magnetohydrodynamic free convection along a vertical wavy surface. They also investigated combined heat and mass transfer in natural convection flow from a vertical wavy surface in the year of 1999. Wang and Chen (2001) investigated the effects of transient force and free convection along a vertical wavy surface in micropolar fluid. Chamkha (2002) analyzed the effects of magnetic field and heat generation/absorption on natural convection from an isothermal surface in a stratified environment. Hossain et al. (2002) studied natural convection of fluid with variable viscosity from a heated vertical wavy surface. Furthermore Jang et al. (2003) studied natural convection heat and mass transfer along a vertical wavy surface. Natural convection flow along a vertical wavy surface with uniform surface temperature in presence of heat generation/absorption is investigated by Molla and Hossain (2004). They also investigated radiation effect on mixed convection laminar flow along a vertical wavy surface in the year of 2007. Chamkha et al. (2006) studied effects of heat generation or absorption on thermophoretic free convection boundary layer from a vertical flat plate embedded in a porous medium. (2007): Viscous dissipation effects on MHD natural convection flow over a sphere in the presence of heat generation are investigated by Alam et al. (2007). Mamun et al. (2008) studied MHD–conjugate heat transfer analysis for a vertical



flat plate in presence of viscous dissipation and heat generation. Azim et al. (2010) analyzed viscous Joule heating MHD conjugate heat transfer for a vertical flat plate in the presence of heat generation. In the same year Anjali and Kayalvizhi (2010) studied viscous dissipation and radiation effects on the thermal boundary layer flow with heat and mass transfer over a non-isothermal stretching sheet with internal heat generation embedded in a porous medium. Jha and Ajibade (2011) showed the effect of viscous dissipation on natural convection flow between vertical parallel plates with time-periodic boundary conditions. Palani and Kim (2011) studied on Joule heating and viscous dissipation effects on MHD flow past a semi-infinite inclined plate with variable surface temperature. Effect of temperature-dependent variable viscosity on magnetohydrodynamic natural convection flow along a vertical wavy surface are investigated by Parveen and Alim (2011). They also analyzed MHD free convection flow along a vertical wavy surface with temperature dependent thermal conductivity in presence of heat generation (2012). Parveen and Alim (2013) also studied Joule heating and MHD free convection flow along a vertical wavy surface with viscosity and thermal conductivity dependent on temperature. Numerical solution of temperature dependent thermal conductivity on MHD free convection flow with joule heating along a vertical wavy surface is also investigated by Parveen and Alim (2014).

## 1.2 Main Objectives of the Present Works

The aim of this research is to investigate the effects of viscous dissipation and Joule heating on natural convection flow in presence of heat generation along a vertical wavy surface. The stream is assumed to flow in the upward vertical direction. Here the surface temperature  $T_w$  is higher than the ambient temperature  $T_\infty$ . Solutions will be obtained and analyzed for the velocity and temperature profiles, the streamlines and isotherms patterns, the surface shear stress in terms of the local skin friction coefficient and the rate of heat transfer in terms of local Nusselt number over the whole boundary layer for a selection of parameters set consisting of viscous dissipation parameter, magnetic field parameter, Joule heating parameter, heat generation parameter, the amplitude of the waviness of the surface and Prandtl number.

The major objectives of this study are:

- To derive the governing equations regarding the proposed study.
- To reduce the governing equations into a system of ordinary differential equations using suitable transformations.
- To solve the system of ordinary differential equations numerically with the help of implicit finite difference method together with the Keller-Box scheme.
- To investigate the effects of dimensionless parameters namely viscous dissipation parameter  $Ec$ , heat generation parameter  $Q$ , magnetic parameter  $M$ , Joule heating parameter  $J$ , Prandtl number  $Pr$  and amplitude-to-length ratio  $\alpha$  of the wavy surface.
- To present the numerical results graphically for different values of the parameters entering into the present study.
- To compare the present results with other published works.

### 1.3 Outline of Methodology

There are generally three types of numerical techniques depending on the types of problem to be solved. They are (i) Finite Element (ii) Finite Difference and (iii) Finite Volume Method. The Finite Difference Method is very efficient for programming and rapid convergence. The transformed boundary layer equations are solved numerically with the help of implicit finite difference method together with the Keller-box scheme (1978), which has been in details by Cebeci and Bradshaw (1984). The momentum and energy equations are first converted into a system of first order differential equations. Then these equations are expressed in finite difference forms by approximating the functions and their derivatives in terms of the center differences. Denoting the mesh points in the  $x$  and  $\eta$ -plane by  $x_i$  and  $\eta_j$  where  $i = 1, 2, \dots, M$  and  $j = 1, 2, \dots, N$ , central difference approximations are made, such that those equations involving  $x$  explicitly are centered at  $(x_{i-1/2}, \eta_{j-1/2})$  and the remainder at  $(x_i, \eta_{j-1/2})$ , where  $\eta_{j-1/2} = 1/2(\eta_j + \eta_{j-1})$  etc. The above central difference approximations reduces the system of first order differential equations to a set of non-linear difference equations for the unknown at  $x_i$  in terms of their values at  $x_{i-1}$ . The resulting set of non-linear difference equations are solved by using the Newton's quasi-linearization method. The Jacobian matrix has a block-tridiagonal structure and the difference equations are solved using a block-matrix version of the Thomas algorithm. The whole procedure namely reduction to first order followed by central difference approximations, Newton's Quasi-linearization method and the block Thomas algorithm, is well known as Keller-box method.

Effects of various parameters on the velocity and temperature profiles, the surface shear stress in terms of the skin friction coefficient, the rate of heat transfer in terms of local Nusselt number, the streamlines as well as the isotherms are shown graphically for different values of parameters entering into the problem using the post processing software TECPLOT and also in tabular form.

# Chapter Two

## Mathematical modeling of the flow problem

---

### Why did magnetic parameter include in this work?

*As the Joule heating effects are being investigated with heat generation and viscous dissipation along a vertical wavy surface it is necessary to form equations including magnetic parameter because Joule heating effects and Magnetic effects on fluid flow are interrelated. Here magnetic effect tries to oppose velocity of fluid increased by Joule heating in vertical direction.*

### 2.1 Governing equations of the flow

Magnetohydrodynamic equations are the ordinary electromagnetic and hydrodynamic equations modified to take account of the interaction between the motion of the fluid and electromagnetic field. Formulation of electromagnetic theory in mathematical form is known as Maxwell's equations. Maxwell's basic equations show the relation of basic field quantities and their production. But it is assumed that all velocities are small in comparison with the speed of light. Before writing down the MHD equations it is essential to know about the ordinary electromagnetic equations and hydromagnetic equations, which are as follows (see Cramer and Pai (1974)).

$$\text{Charge Continuity:} \quad \nabla \cdot \vec{D} = \rho_e \quad (2.1)$$

$$\text{Current Continuity:} \quad \nabla \cdot \vec{J} = -\frac{\partial \rho_e}{\partial t} \quad (2.2)$$

$$\text{Magnetic field continuity:} \quad \nabla \cdot \vec{B} = 0 \quad (2.3)$$

$$\text{Ampere's Law:} \quad \nabla \wedge \beta_0 = \vec{J} + \frac{\partial \vec{D}}{\partial t} \quad (2.4)$$

$$\text{Faraday's Law:} \quad \nabla \wedge \vec{E} = -\frac{\partial \vec{B}}{\partial t} \quad (2.5)$$

$$\text{Constitutive equations for D and B: } \vec{D} = \epsilon' \vec{E} \text{ and } \vec{B} = \mu_e \beta_0 \quad (2.6)$$

Total current density flow: 
$$\vec{J} = \sigma_0 (\vec{E} + \vec{q} \wedge \vec{B}) + \rho_e \vec{q} \quad (2.7)$$

The above equations (2.1) to (2.7) are Maxwell's equations where  $\vec{D}$  is the electron displacement,  $\rho_e$  is the charge density,  $\vec{E}$  is the electric field,  $\vec{B}$  is the magnetic field,  $\beta_0$  is the magnetic field strength,  $\vec{J}$  is the current density,  $\partial\vec{D}/\partial t$  is the displacement current density,  $\epsilon'$  is the electric permeability of the medium,  $\mu_e$  is the magnetic permeability of the medium,  $\vec{q}$  is the vector field and  $\sigma_0$  is the electric conductivity.

The electromagnetic equations as shown above are not usually applied in their present form and require interpretation and several assumptions to provide the set to be used in MHD. In MHD a fluid is considered that is grossly neutral. The charge density  $\rho_e$  in Maxwell's equations must then be interpreted, as an excess charge density, which is generally not large. If it is disregard the excess charge density then it must disregard the displacement current. In most problems the displacement current, the excess charge density and the current due to convection of the excess charge are small. Taking into this effect the electromagnetic equations can be reduced to the following form:

$$\nabla \cdot \vec{D} = 0 \quad (2.8)$$

$$\nabla \cdot \vec{J} = 0 \quad (2.9)$$

$$\nabla \cdot \vec{B} = 0 \quad (2.10)$$

$$\nabla \wedge \beta_0 = \vec{J} \quad (2.11)$$

$$\nabla \wedge \vec{E} = - \frac{\partial \vec{B}}{\partial t} \quad (2.12)$$

$$\vec{D} = \epsilon' \vec{E} \text{ and } \vec{B} = \mu_e \beta_0 \quad (2.13)$$

$$\vec{J} = \sigma_0 (\vec{E} + \vec{q} \wedge \vec{B}) \quad (2.14)$$

Below we shall now suitably represent the equations of fluid dynamics to take account of the electromagnetic phenomena.

### The continuity equation

The MHD continuity equation for viscous incompressible electrically conducting fluid remains same as that of usual continuity equation  $\nabla \cdot \vec{q} = 0$  (2.15)

### The Navier-Stokes equation

The motion of the conducting fluid across the magnetic field generates electric currents, which change the magnetic field and the action of the magnetic field on these current give rises to mechanical forces, which modify the flow of the fluid. Thus, the fundamental equation of the magneto-fluid combines the equations of the motion from fluid mechanics with Maxwell's equations from electrodynamics.

Then the Navier-stokes equation for a viscous incompressible fluid may be written in the following form:

$$\rho(\vec{q} \cdot \nabla)\vec{q} = -\nabla P + \mu \nabla^2 \vec{q} + \vec{F} + \vec{J} \times \vec{B} \quad (2.16)$$

Where  $\rho$  is the fluid density,  $\mu$  is the viscosity and  $P$  is the pressure. The first term on the right hand side of equation (2.16) is the pressure gradient, second term is the viscosity, third term is the body force per unit volume and last term is the electromagnetic force due to motion of the fluid.

### The energy equation

The energy equation for a viscous incompressible fluid is obtained by adding the electromagnetic energy term into the classical gas dynamic energy equation. This equation can be written as

$$\rho C_p (\vec{q} \cdot \nabla) T = \nabla \cdot (k \nabla T) + \nu \nabla^2 u + \mu \nabla^2 \vec{q} \quad (2.17)$$

Where,  $k$  is the thermal conductivity,  $C_p$  is the specific heat with constant pressure. In the physical problem of temperature variation,  $u(x,y,z,t)$  is the temperature and  $\nu$  is the thermal diffusivity. For the mathematical treatment it is sufficient to consider the case  $\nu = 1$ . The left side of equation (2.17) represents the net energy transfer due to mass transfer, the first term on the right hand side represents conductive heat transfer and second term is heat generation term and third term is for viscous dissipation term.

Where  $\vec{q} = (U, V)$ ,  $U$  and  $V$  are the velocity components along the X and Y axes respectively,  $\vec{F}$  is the body force per unit volume which is defined as  $-\rho g$ , the terms  $\vec{J}$  and  $\vec{B}$  are respectively the current density and magnetic induction vector and the term  $\vec{J} \times \vec{B}$  is the force on the fluid per unit volume produced by the interaction of the current and magnetic field in the absence of excess charges,  $T$  is the temperature of the fluid in the boundary layer,  $g$  is the acceleration due to gravity,  $k$  is the thermal conductivity and  $C_P$  is the specific heat at constant pressure and  $\mu$  is the viscosity of the fluid.

Here  $\vec{B} = \mu_e \beta_0$ ,  $\mu_e$  being the magnetic permeability of the fluid,  $\beta_0$  is the uniformly distributed transverse magnetic field of strength and  $\nabla$  is the vector differential operator and is defined for two dimensional case as

$$\nabla = \hat{l}_x \frac{\partial}{\partial x} + \hat{l}_y \frac{\partial}{\partial y}$$

where  $\hat{l}_x$  and  $\hat{l}_y$  are the unit vector along x and y axes respectively. When the external electric field is zero and the induced electric field is negligible, the current density is related to the velocity by Ohm's law as follows

$$\vec{J} = \sigma_0 (\vec{q} \times \vec{B}) \quad (2.18)$$

where  $(\vec{q} \times \vec{B})$  is electrical fluid vector and  $\sigma_0$  denotes the electric conductivity of the fluid.

Under the conduction that the magnetic Reynolds number is small, the induced magnetic field is negligible compared with applied field. This condition is well satisfied in terrestrial applications, especially so in (low velocity) free convection flows. So it can be written as

$$\vec{B} = \hat{l}_y \beta_0 \quad (2.19)$$

Bringing together equations (2.18) and (2.19) the force per unit volume  $\vec{J} \times \vec{B}$  acting along the x-axis takes the following form

$$\vec{J} \times \vec{B} = -\sigma_0 \beta_0^2 U \quad (2.20)$$

The steady two dimensional laminar free convection boundary layer flow of a viscous incompressible and electrically conducting fluid along a vertical wavy surface in presence of viscous dissipation and heat generation with uniform transverse magnetic field of strength  $\beta_0$  is considered. It is assumed that the wavy surface is electrically insulated and is maintained at a uniform temperature  $T_w$ . Far above the wavy plate, the fluid is stationary and is kept at a

temperature  $T_\infty$ , where  $T_w > T_\infty$ .

The boundary layer analysis outlined below allows  $\bar{\sigma}(X)$  being arbitrary, but our detailed numerical work assumed that the surface exhibits sinusoidal deformations. The wavy surface may be described by

$$Y_w = \bar{\sigma}(X) = \alpha \sin\left(\frac{n\pi X}{L}\right) \quad (2.21)$$

where  $L$  is the characteristic wave length associated with the wavy surface.

The geometry of the wavy surface and the two-dimensional cartesian coordinate system are shown in figure 2.1.

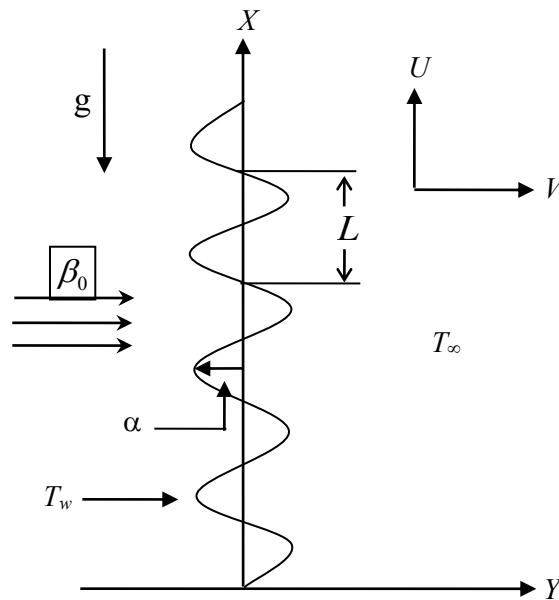


**Figure 2.1:** The coordinate system and the physical model.

Under the usual Boussinesq approximation, we consider the flow governed by the following boundary equations:

Continuity Equation

$$\frac{\partial U}{\partial X} + \frac{\partial V}{\partial Y} = 0 \quad (2.22)$$

Momentum Equations



$$\text{X- momentum: } U \frac{\partial U}{\partial X} + V \frac{\partial U}{\partial Y} = -\frac{1}{\rho} \frac{\partial P}{\partial X} + \nu \nabla^2 U + g\beta(T - T_\infty) - \frac{\sigma_0 \beta_0^2}{\rho} U \quad (2.23)$$

$$\text{Y- momentum: } U \frac{\partial V}{\partial X} + V \frac{\partial V}{\partial Y} = -\frac{1}{\rho} \frac{\partial P}{\partial Y} + \nu \nabla^2 V \quad (2.24)$$

$$\text{Energy equation: } U \frac{\partial T}{\partial X} + V \frac{\partial T}{\partial Y} = \frac{\nu}{\rho C_p} \nabla^2 T + \frac{\nu}{\rho C_p} (T - T_\infty) + \frac{k}{C_p} \left( \frac{\partial T}{\partial Y} \right) + \frac{\sigma_0}{\rho C_p} U \quad (2.25)$$

Where  $(X, Y)$  are the dimensional coordinates along and normal to the tangent of the surface and  $(U, V)$  are the velocity components parallel to  $(X, Y)$ ,  $\nabla^2 (= \partial^2/\partial x^2 + \partial^2/\partial y^2)$  is the Laplacian operator,  $g$  is the accelerate on due to gravity,  $P$  is the dimensional pressure of the fluid,  $\rho$  is the density,  $C_p$  is the specific heat at constant at constant pressure and  $\nu (= \mu/\rho)$  is the kinematic viscosity and  $\mu$  is the dynamic viscosity,  $k$  is the thermal conductivity of the fluid in the boundary region depending on the fluid temperature,  $\sigma_0$  is the electrical conductivity of the fluid and  $\beta$  is the volumetric coefficient of thermal expansion.

The boundary conditions for the present problem are

$$U = V = 0, T = T_w \quad \text{at } Y = 0 \quad (2.26)$$

$$U = 0, T = T_\infty, P = P_\infty \quad \text{as } Y \rightarrow \infty \quad (2.27)$$

Where  $T_w$  is the surface temperature,  $T_\infty$  is the ambient temperature of the fluid and  $P_\infty$  is the pressure of the fluid outside the boundary layer.

## 2.2 Transformation of the governing equations

Using Prandtl's transposition theorem to transform the irregular wavy surface into a flat surface as extended by Yao (1988) and boundary-layer approximation, the following dimensionless variables are introduced for non-dimensionalizing the governing equations,

$$\begin{aligned}
 x &= \frac{X}{L}, \quad y = \frac{Y - \bar{\sigma}}{L} Gr^{\frac{1}{4}}, \quad p = \frac{L^2}{\rho v^2} Gr^{-1} P \\
 u &= \frac{L}{v} Gr^{-\frac{1}{2}} U, \quad v = \frac{L}{v} Gr^{-\frac{1}{4}} (V - \sigma_x U) \\
 \theta &= \frac{T - T_\infty}{T_w - T_\infty}, \quad \sigma_x = \frac{d\bar{\sigma}}{dX} = \frac{d\sigma}{dx}, \quad Gr = \frac{g\beta(T_w - T_\infty)L^3}{v^2}
 \end{aligned} \tag{2.28}$$

Where  $\theta$  is the non-dimensional temperature function and  $(u, v)$  are the dimensionless velocity components parallel to  $(x, y)$ . Here  $(x, y)$  are not orthogonal, but a regular rectangular computational grid can be easily fitted in the transformed coordinates. It is also worthwhile to point out that  $(u, v)$  are the velocity components parallel to  $(x, y)$  which are not parallel to the wavy surface.

The conservation equations for the flow characterized with steady, laminar and two-dimensional boundary layer; under the usual Boussinesq approximation, dimensionless form of the continuity, momentum and energy equations can be written as:

$$\frac{\partial u}{\partial x} + \frac{\partial v}{\partial y} = 0 \tag{2.29}$$

$$u \frac{\partial u}{\partial x} + v \frac{\partial u}{\partial y} = -\frac{\partial p}{\partial x} + Gr^{\frac{1}{4}} \sigma_x \frac{\partial p}{\partial y} + (1 + \sigma_x^2) \frac{\partial^2 u}{\partial y^2} - Mu + \theta \tag{2.30}$$

$$\sigma_x \left( u \frac{\partial u}{\partial x} + v \frac{\partial u}{\partial y} \right) = -Gr^{\frac{1}{4}} \frac{\partial p}{\partial y} + \sigma_x (1 + \sigma_x^2) \frac{\partial^2 u}{\partial y^2} - \sigma_{xx} u^2 \tag{2.31}$$

$$u \frac{\partial \theta}{\partial x} + v \frac{\partial \theta}{\partial y} = \frac{1}{Pr} (1 + \sigma_x^2) \frac{\partial^2 \theta}{\partial y^2} + Q\theta + Ec \left( \frac{\partial u}{\partial y} \right)^2 + Ju^2 \tag{2.32}$$

Where  $Pr = \frac{C_p \mu}{k}$  is the Prandtl number,  $Q = \frac{Q_0 L^2}{\mu C_p Gr^{1/2}}$  is the heat generation/absorption parameter,  $Ec = \frac{\nu^2 Gr}{L^2 C_p (T_w - T_\infty)}$  is the viscous dissipation parameter,  $J = \frac{\sigma_0 \beta_0^2 \nu Gr^{1/2}}{\rho C_p (T_w - T_\infty)}$  is the Joule heating parameter and  $M = \frac{\sigma_0 \beta_0^2 L^2}{\mu Gr^{1/2}}$  is the magnetic parameter.

It can easily be seen that the convection induced by the wavy surface is described by equations (2.29)–(2.32). We further notice that, equation (2.31) indicates that the pressure gradient along the y-direction is  $O(Gr^{-1/4})$ , which implies that lowest order pressure gradient along x -direction can be determined from the inviscid flow solution. For the present problem this pressure gradient ( $\partial p / \partial x = 0$ ) is zero. Equation (2.31) further shows that  $Gr^{1/4} \partial p / \partial y$  is  $O(1)$  and is determined by the left-hand side of this equation. Thus, the elimination of  $\partial p / \partial y$  from equations (2.30) and (2.31) leads to

$$\frac{\partial}{\partial x} \left( \nu \frac{\partial u}{\partial y} - (\nu \sigma_x) \frac{\partial u}{\partial y^2} - \frac{\nu}{1 + \sigma_x^2} u - \frac{\nu}{1 + \sigma_x^2} u + \frac{\nu}{1 + \sigma_x^2} \nu \right) \quad (2.33)$$

The corresponding boundary conditions for the present problem are:

$$\left. \begin{aligned} u = v = 0, \quad \theta = 1 & \quad \text{at } y = 0 \\ u = \theta = 0, \quad p = 0 & \quad \text{as } y \rightarrow \infty \end{aligned} \right\} \quad (2.34)$$

Now we introduce the following transformations to reduce the governing equations to a convenient form:

$$\psi = x^{3/4} f(x, \eta), \quad \eta = yx^{-1/4}, \quad \theta = \theta(x, \eta) \quad (2.35)$$

where  $f(\eta)$  is the dimensionless stream function,  $\eta$  is the pseudo similarity variable and  $\psi$  is the stream function that satisfies the equation (2.29).

Introducing the transformations given in equation (2.35) and into equations (2.32) and (2.33) the following system of non linear equations are obtained,

$$(1 + \sigma_x^2) f''' + \frac{3}{4} f f'' - \left( \frac{1}{2} + \frac{x \sigma_x \sigma_{xx}}{1 + \sigma_x^2} \right) f'^2 + \frac{1}{1 + \sigma_x^2} \theta - \frac{Mx^{1/2}}{1 + \sigma_x^2} f' = x \left( f' \frac{\partial f'}{\partial x} - f'' \frac{\partial f}{\partial x} \right) \quad (2.36)$$

$$\frac{1}{\text{Pr}}(1+\sigma_x^2)\theta'' + \frac{3}{4}f\theta' + x^{\frac{1}{2}}Q\theta + Ecxf''^2 + Jx^{\frac{3}{2}}f'^2 = x\left(f'\frac{\partial\theta}{\partial x} - \theta\frac{\partial f}{\partial x}\right) \quad (2.37)$$

The boundary conditions (2.34) now take the following form:

$$\left. \begin{aligned} f(x,0) = f'(x,0) = 0, \quad \theta(x,0) = 1 \\ f'(x,\infty) = 0, \quad \theta(x,\infty) = 0 \end{aligned} \right\} \quad (2.38)$$

In the above equations prime denote the differentiation with respect to  $\eta$ .

The local skin friction coefficient  $C_{fx}$  and the rate of heat transfer in terms of the local Nusselt number  $Nu_x$  takes the following form:

$$C_{fx}(Gr/x)^{1/4}/2 = \sqrt{1+\sigma_x^2} f''(x,0) \quad (2.39)$$

$$Nu_x(Gr/x)^{-1/4} = -\sqrt{1+\sigma_x^2} \theta'(x,0) \quad (2.40)$$

## 2.3 Implicit Finite Difference Method (IFDM)

To apply the aforementioned method, equations (2.36) and (2.37) their boundary condition (2.38) are first converted into the following system of first order equations. For this purpose we introduce new dependent variables  $u(\xi,\eta)$ ,  $v(\xi,\eta)$ ,  $p(\xi,\eta)$  and  $g(\xi,\eta)$  so that the transformed momentum and energy equations can be written as:

$$f' = u \quad (2.41)$$

$$u' = v \quad (2.42)$$

$$g' = p \quad (2.43)$$

$$P_1v' + P_2fv - P_3u^2 + P_4g - P_5u = \xi\left(u\frac{\partial u}{\partial \xi} - v\frac{\partial f}{\partial \xi}\right) \quad (2.44)$$

$$\frac{1}{\text{Pr}}P_1p' + P_2fp + P_6v^2 + P_7g + P_8u^2 = \xi\left(u\frac{\partial g}{\partial \xi} - p\frac{\partial f}{\partial \xi}\right) \quad (2.45)$$

where  $x = \xi$ ,  $\theta = g$  and

$$P_1 = (1 + \sigma_x^2), P_2 = \frac{3}{4}, P_3 = \frac{1}{2} + \frac{x\sigma_x\sigma_{xx}}{1 + \sigma_x^2}, P_4 = \frac{1}{1 + \sigma_x^2}, P_5 = \frac{Mx^{1/2}}{1 + \sigma_x^2},$$

$$P_6 = Ecx, P_7 = x^{1/2}Q, P_8 = Jx^{3/2}$$

and the boundary conditions (2.38) are

$$f(\xi, 0) = 0, u(\xi, 0) = 0, g(\xi, 0) = 1$$

$$u(\xi, \infty) = 0, g(\xi, \infty) = 0$$

(2.46)

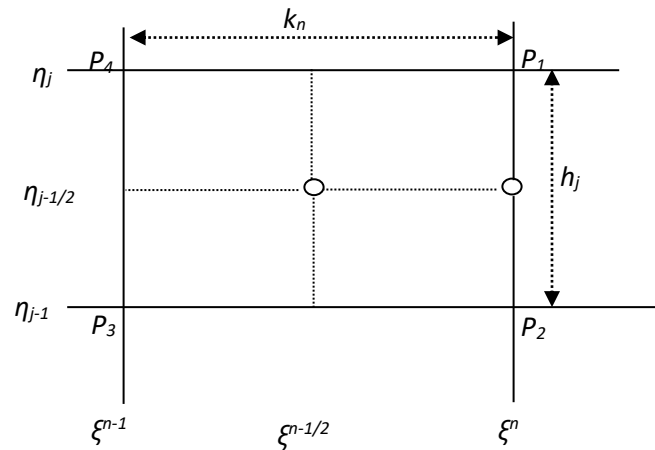


**Figure 2.2:** Net rectangle of difference approximations for the Box scheme.

Now consider the net rectangle on the  $(\xi, \eta)$  plane shown in the figure (2.2) and denote the net points by

$$\xi^0 = 0, \xi^n = \xi^{n-1} + k_n, n = 1, 2, \dots, N$$

$$\eta_0 = 0, \eta_j = \eta_{j-1} + h_j, j = 1, 2, \dots, J$$

(2.47)

Here  $n$  and  $j$  are just sequence of numbers on the  $(\xi, \eta)$  plane,  $k_n$  and  $h_j$  are the variable mesh widths. Approximate the quantities  $f, u, v$  and  $p$  at the points  $(\xi^n, \eta_j)$  of the net by

$f_j^n, u_j^n, v_j^n, p_j^n$  which call net function. It is also employed that the notation  $P_j^n$  for the quantities midway between net points shown in figure (2.2) and for any net function as

$$\xi^{n-1/2} = \frac{1}{2}(\xi^n + \xi^{n-1}) \quad (2.48)$$

$$\eta_{j-1/2} = \frac{1}{2}(\eta_j + \eta_{j-1}) \quad (2.49)$$

$$g_j^{n-1/2} = \frac{1}{2}(g_j^n + g_j^{n-1}) \quad (2.50)$$

$$g_{j-1/2}^n = \frac{1}{2}(g_j^n + g_{j-1}^n) \quad (2.51)$$

The finite difference approximations according to box method to the three first order ordinary differential equations (2.41) – (2.43) are written for the midpoint  $(\xi^n, \eta_{j-1/2})$  of the segment  $P_1P_2$  shown in the figure (2.2) and the finite difference approximations to the two first order differential equations (2.44) and (2.45) are written for the midpoint  $(\xi^{n-1/2}, \eta_{j-1/2})$  of the rectangle  $P_1P_2P_3P_4$ . This procedure yields

$$\frac{f_j^n - f_{j-1}^n}{h_j} = u_{j-1/2}^n = \frac{u_{j-1}^n + u_j^n}{2} \quad (2.52)$$

$$\frac{u_j^n - u_{j-1}^n}{h_j} = v_{j-1/2}^n = \frac{v_{j-1}^n + v_j^n}{2} \quad (2.53)$$

$$\frac{g_j^n - g_{j-1}^n}{h_j} = p_{j-1/2}^n = \frac{p_{j-1}^n + p_j^n}{2} \quad (2.54)$$

$$\frac{1}{2}(P_1T)_{j-1/2}^n \left( \frac{v_j^n - v_{j-1}^n}{h_j} \right) + \frac{1}{2}(P_1T)_{j-1/2}^{n-1} \left( \frac{v_j^{n-1} - v_{j-1}^{n-1}}{h_j} \right) + (P_2fv)_{j-1/2}^{n-1/2} - (P_3u^2)_{j-1/2}^{n-1/2} \quad (2.55)$$

$$+ (P_4g)_{j-1/2}^{n-1/2} - (P_5u)_{j-1/2}^{n-1/2} = \xi_{j-1/2}^{n-1/2} \left( u_{j-1/2}^{n-1/2} \frac{u_{j-1/2}^n - u_{j-1/2}^{n-1}}{k_n} - v_{j-1/2}^{n-1/2} \frac{f_{j-1/2}^n - f_{j-1/2}^{n-1}}{k_n} \right)$$

$$\frac{1}{2Pr} \left\{ (P_1)_{j-1/2}^n \right\} \left( \frac{p_j^n - p_{j-1}^n}{h_j} \right) + \frac{1}{2Pr} \left\{ (P_1)_{j-1/2}^{n-1} \right\} \left( \frac{p_j^{n-1} - p_{j-1}^{n-1}}{h_j} \right) + (P_2fp)_{j-1/2}^{n-1/2} \quad (2.56)$$

$$+ (P_6v^2)_{j-1/2}^{n-1/2} + (P_7g)_{j-1/2}^{n-1/2} + (P_8u^2)_{j-1/2}^{n-1/2}$$

$$= \xi_{j-1/2}^{n-1/2} \left( u_{j-1/2}^{n-1/2} \frac{g_{j-1/2}^n - g_{j-1/2}^{n-1}}{k_n} - p_{j-1/2}^{n-1/2} \frac{f_{j-1/2}^n - f_{j-1/2}^{n-1}}{k_n} \right)$$

Now the equation (2.55) can be written as

$$\begin{aligned}
 &\Rightarrow \frac{1}{2}(P_1 T)_{j-1/2}^n \left( \frac{v_j^n - v_{j-1}^n}{h_j} \right) + \frac{1}{2}(P_1 T)_{j-1/2}^{n-1} \left( \frac{v_j^{n-1} - v_{j-1}^{n-1}}{h_j} \right) + \frac{1}{2} \{ (P_2 f v)_{j-1/2}^n + (P_2 f v)_{j-1/2}^{n-1} \} \\
 &- \frac{1}{2} \{ (P_3 u^2)_{j-1/2}^n + (P_3 u^2)_{j-1/2}^{n-1} \} + \frac{1}{2} \{ (P_4 g)_{j-1/2}^n + (P_4 g)_{j-1/2}^{n-1} \} - \frac{1}{2} \{ (P_5 u)_{j-1/2}^n + (P_5 u)_{j-1/2}^{n-1} \} \\
 &= \frac{1}{2k_n} \xi_{j-1/2}^{n-1/2} (u_{j-1/2}^n + u_{j-1/2}^{n-1}) (u_{j-1/2}^n - u_{j-1/2}^{n-1}) - \frac{1}{2k_n} \xi_{j-1/2}^{n-1/2} (v_{j-1/2}^n + v_{j-1/2}^{n-1}) (f_{j-1/2}^n - f_{j-1/2}^{n-1}) \\
 &\Rightarrow (P_1 T)_{j-1/2}^n \left( \frac{v_j^n - v_{j-1}^n}{h_j} \right) + (P_1 T)_{j-1/2}^{n-1} \left( \frac{v_j^{n-1} - v_{j-1}^{n-1}}{h_j} \right) + (P_2)_{j-1/2}^n (f v)_{j-1/2}^n + (P_2)_{j-1/2}^{n-1} (f v)_{j-1/2}^{n-1} \\
 &- (P_3)_{j-1/2}^n (u^2)_{j-1/2}^n - (P_3)_{j-1/2}^{n-1} (u^2)_{j-1/2}^{n-1} + (P_4)_{j-1/2}^n g_{j-1/2}^n + (P_4)_{j-1/2}^{n-1} g_{j-1/2}^{n-1} - (P_5)_{j-1/2}^n (u)_{j-1/2}^n \\
 &- (P_5)_{j-1/2}^{n-1} (u)_{j-1/2}^{n-1} = \alpha_n \{ (u^2)_{j-1/2}^n - (u^2)_{j-1/2}^{n-1} - (f v)_{j-1/2}^n + f_{j-1/2}^{n-1} v_{j-1/2}^n - f_{j-1/2}^n v_{j-1/2}^{n-1} + (f v)_{j-1/2}^{n-1} \} \\
 &\Rightarrow (P_1 T)_{j-1/2}^n \left( \frac{v_j^n - v_{j-1}^n}{h_j} \right) + \{ (P_2)_{j-1/2}^n + \alpha_n \} (f v)_{j-1/2}^n - \{ (P_3)_{j-1/2}^n + \alpha_n \} (u^2)_{j-1/2}^n \\
 &+ (P_4)_{j-1/2}^n g_{j-1/2}^n - (P_5)_{j-1/2}^n (u)_{j-1/2}^n = \alpha_n \left[ - (u^2)_{j-1/2}^{n-1} + v_{j-1/2}^n f_{j-1/2}^{n-1} - f_{j-1/2}^n v_{j-1/2}^{n-1} + (f v)_{j-1/2}^{n-1} \right] \\
 &- (P_2)_{j-1/2}^{n-1} (f v)_{j-1/2}^{n-1} + (P_3)_{j-1/2}^{n-1} (u^2)_{j-1/2}^{n-1} - (P_4)_{j-1/2}^{n-1} g_{j-1/2}^{n-1} + (P_5)_{j-1/2}^{n-1} (u)_{j-1/2}^{n-1} \\
 &- (P_1 T)_{j-1/2}^{n-1} \left( \frac{v_j^{n-1} - v_{j-1}^{n-1}}{h_j} \right) \\
 &R_{j-1/2}^{n-1} = \alpha_n \{ (f v)_{j-1/2}^{n-1} - (u^2)_{j-1/2}^{n-1} \} - L_{j-1/2}^{n-1} \tag{2.57}
 \end{aligned}$$

$$\text{where } \alpha_n = \frac{1}{k_n} \xi_{j-1/2}^{n-1/2} \tag{2.58}$$

$$\begin{aligned}
 &\Rightarrow (P_1 T)_{j-1/2}^n h_j^{-1} (v_j^n - v_{j-1}^n) + \{ (P_2)_{j-1/2}^n + \alpha_n \} (f v)_{j-1/2}^n \\
 &- \{ (P_3)_{j-1/2}^n + \alpha_n \} (u^2)_{j-1/2}^n + (P_4)_{j-1/2}^n g_{j-1/2}^n - (P_5)_{j-1/2}^n (u)_{j-1/2}^n \\
 &+ \alpha_n (f_{j-1/2}^n v_{j-1/2}^{n-1} - v_{j-1/2}^n f_{j-1/2}^{n-1}) = R_{j-1/2}^{n-1} \tag{2.59}
 \end{aligned}$$

$$\begin{aligned}
 &\Rightarrow (P_1 T)_{j-1/2}^{n-1} h_j^{-1} (v_j^{n-1} - v_{j-1}^{n-1}) + (P_2)_{j-1/2}^{n-1} (f v)_{j-1/2}^{n-1} - (P_3)_{j-1/2}^{n-1} (u^2)_{j-1/2}^{n-1} \\
 &+ (P_4)_{j-1/2}^{n-1} g_{j-1/2}^{n-1} - (P_5)_{j-1/2}^{n-1} (u)_{j-1/2}^{n-1} = L_{j-1/2}^{n-1} \tag{2.60}
 \end{aligned}$$

Again from the equation (2.56) then

$$\begin{aligned} & \frac{1}{\text{Pr}} \left[ \left\{ (P_1)_{j-1/2}^n \right\} \left( \frac{p_j^n - p_{j-1}^n}{h_j} \right) + \left\{ (P_1)_{j-1/2}^{n-1} \right\} \left( \frac{p_j^{n-1} - p_{j-1}^{n-1}}{h_j} \right) \right] + \left\{ (P_2 fp)_{j-1/2}^n + (P_2 fp)_{j-1/2}^{n-1} \right\} \\ & + \left\{ (P_6 v^2)_{j-1/2}^n + (P_6 v^2)_{j-1/2}^{n-1} \right\} + \left\{ (P_7 g)_{j-1/2}^n + (P_7 g)_{j-1/2}^{n-1} \right\} + \left\{ (p_8 u^2)_{j-1/2}^n + (p_8 u^2)_{j-1/2}^{n-1} \right\} \\ & = \alpha_n \left[ \left( u_{j-1/2}^n + u_{j-1/2}^{n-1} \right) \left( g_{j-1/2}^n - g_{j-1/2}^{n-1} \right) - \left( p_{j-1/2}^n + p_{j-1/2}^{n-1} \right) \left( f_{j-1/2}^n - f_{j-1/2}^{n-1} \right) \right] \end{aligned}$$

$$\begin{aligned} \Rightarrow & \frac{1}{\text{Pr}} \left\{ (P_1)_{j-1/2}^n \right\} \left( \frac{p_j^n - p_{j-1}^n}{h_j} \right) + \frac{1}{\text{Pr}} \left\{ (P_1)_{j-1/2}^{n-1} \right\} \left( \frac{p_j^{n-1} - p_{j-1}^{n-1}}{h_j} \right) + (P_2)_{j-1/2}^n (fp)_{j-1/2}^n \\ & + (P_2)_{j-1/2}^{n-1} (fp)_{j-1/2}^{n-1} + (P_6)_{j-1/2}^n (v^2)_{j-1/2}^n + (P_6)_{j-1/2}^{n-1} (v^2)_{j-1/2}^{n-1} + (P_7)_{j-1/2}^n (g)_{j-1/2}^n \\ & + (P_7)_{j-1/2}^{n-1} (g)_{j-1/2}^{n-1} + (P_8)_{j-1/2}^n (u^2)_{j-1/2}^n + (P_8)_{j-1/2}^{n-1} (u^2)_{j-1/2}^{n-1} = \alpha_n \\ & \left[ (ug)_{j-1/2}^n - u_{j-1/2}^n g_{j-1/2}^{n-1} + g_{j-1/2}^n u_{j-1/2}^{n-1} - (ug)_{j-1/2}^{n-1} - (fp)_{j-1/2}^n \right] \\ & \left[ + p_{j-1/2}^n f_{j-1/2}^{n-1} - f_{j-1/2}^n p_{j-1/2}^{n-1} + (fp)_{j-1/2}^{n-1} \right] \end{aligned}$$

$$\begin{aligned} \Rightarrow & \frac{1}{\text{Pr}} \left\{ (P_1)_{j-1/2}^n \right\} \left( \frac{p_j^n - p_{j-1}^n}{h_j} \right) + \left\{ (P_2)_{j-1/2}^n + \alpha_n \right\} (fp)_{j-1/2}^n + (P_6)_{j-1/2}^n (v^2)_{j-1/2}^n \\ & + (P_7)_{j-1/2}^n (g)_{j-1/2}^n + (P_8)_{j-1/2}^n (u^2)_{j-1/2}^n - \alpha_n (ug)_{j-1/2}^n \\ & + \alpha_n \left[ u_{j-1/2}^n g_{j-1/2}^{n-1} - g_{j-1/2}^n u_{j-1/2}^{n-1} - p_{j-1/2}^n f_{j-1/2}^{n-1} + f_{j-1/2}^n p_{j-1/2}^{n-1} \right] \\ = & -\frac{1}{\text{Pr}} \left\{ (P_1)_{j-1/2}^{n-1} \right\} \left( \frac{p_j^{n-1} - p_{j-1}^{n-1}}{h_j} \right) - (P_2)_{j-1/2}^{n-1} (fp)_{j-1/2}^{n-1} - (P_6)_{j-1/2}^{n-1} (v^2)_{j-1/2}^{n-1} \\ & - (P_7)_{j-1/2}^{n-1} (g)_{j-1/2}^{n-1} - (P_8)_{j-1/2}^{n-1} (u^2)_{j-1/2}^{n-1} + \alpha_n \left[ (fp)_{j-1/2}^{n-1} - (ug)_{j-1/2}^{n-1} \right] \end{aligned}$$

$$\text{where } T_{j-1/2}^{n-1} = -M_{j-1/2}^{n-1} + \alpha_n \left\{ (fp)_{j-1/2}^{n-1} - (ug)_{j-1/2}^{n-1} \right\} \quad (2.61)$$

$$\text{where, } \alpha_n = \frac{1}{k_n} \xi_{j-1/2}^{n-1/2} \quad (2.62)$$



$$\begin{aligned}
 M_{j-1/2}^{n-1} &= \frac{h_j^{-1}}{\text{Pr}} (P_1)_{j-1/2}^{n-1} \{p_j^{n-1} - p_{j-1}^{n-1}\} + (P_2)_{j-1/2}^{n-1} (fp)_{j-1/2}^{n-1} \\
 &+ (P_6)_{j-1/2}^{n-1} (v^2)_{j-1/2}^{n-1} + (P_7)_{j-1/2}^{n-1} (g)_{j-1/2}^{n-1} + (P_8)_{j-1/2}^{n-1} (u^2)_{j-1/2}^{n-1}
 \end{aligned} \tag{2.63}$$

$$\begin{aligned}
 \Rightarrow T_{j-1/2}^{n-1} &= \frac{1}{\text{Pr}} (P_1)_{j-1/2}^n h_j^{-1} (p_j^n - p_{j-1}^n) + \{(P_2)_{j-1/2}^n + \alpha_n\} (fp)_{j-1/2}^n \\
 &+ (P_6)_{j-1/2}^n (v^2)_{j-1/2}^n + (P_7)_{j-1/2}^n (g)_{j-1/2}^n + (P_8)_{j-1/2}^n (u^2)_{j-1/2}^n - \alpha_n (ug)_{j-1/2}^n \\
 &+ \alpha_n (u_{j-1/2}^n g_{j-1/2}^{n-1} - g_{j-1/2}^n u_{j-1/2}^{n-1}) - \alpha_n (p_{j-1/2}^n f_{j-1/2}^{n-1} - f_{j-1/2}^n p_{j-1/2}^{n-1})
 \end{aligned} \tag{2.64}$$

The boundary condition becomes

$$\begin{aligned}
 f_0^n &= 0, \quad u_0^n = 0, \quad g_0^n = 1 \\
 u_j^n &= 0, \quad g_j^n = 0
 \end{aligned} \tag{2.65}$$

# Chapter Three

## Effects of Viscous Dissipation on Free Convection Flow along a Vertical Wavy Surface in presence of Heat Generation

---

### 3.1 Introduction

This chapter describes the effects of viscous dissipation and Joule heating on free convection flow along a vertical wavy surface in presence of heat generation. The governing boundary layer equations with associated boundary conditions are converted to non-dimensional boundary layer equations using the appropriate transformation and the resulting nonlinear system of partial differential equations are reduced to local non similarity equations which are solved numerically by employing the implicit finite difference method, known as Keller-Box scheme.

The effects of the pertinent parameters, such as the heat generation parameter ( $Q$ ) where the amount of heat generation constant  $Q > 0$ , the magnetic parameter ( $M$ ), the Joule heating parameter ( $J$ ) the viscous dissipation parameter ( $Ec$ ), the Prandtl number ( $Pr$ ) and the amplitude of the wavy surface ( $\alpha$ ) on the surface shear stress in terms of the skin friction coefficient  $C_{fx}$ , the rate of heat transfer in terms of Nusselt number  $Nu_x$ , the velocity profiles, the temperature profiles, the streamlines as well as the isotherms are shown graphically.

### 3.2 Results and discussion

Here I have shown the combined effects of viscous dissipation, Joule heating and heat generation on natural convection flow of viscous incompressible fluid along a vertical wavy surface. The velocity profiles, the temperature profiles, the skin friction coefficient  $C_{fx}$ , the rate of heat transfer in terms of Nusselt number  $Nu_x$ , the streamlines as well as the isotherms are shown graphically in figures (3.1) to (3.24) for different values of the heat generation parameter  $Q$  ( $=0.3$  to  $1.0$ ), the Joule heating parameter  $J$  ( $=0.001$  to  $0.040$ ), the Magnetic parameter  $M$  ( $=0.0$  to  $3.0$ ), the viscous dissipation parameter  $Ec$  ( $=0.50$  to  $5.0$ ), the Prandtl number  $Pr$  ( $=0.73, 1.73, 4.24, 7.0$ ) which correspond to the air at  $2100^\circ\text{K}$ , water at  $100^\circ\text{C}$ ,

60°C and 20°C respectively and the amplitude of the wavy surface ranging from  $\alpha = 0.0$  (flat plate) to 0.3 .

### **Velocity and Temperature Profile**

Figure 3.1(a) and (b) represent the velocity and temperature profiles for heat generation parameter  $Q = (0.30, 0.50, 0.70, 1.0)$  while Prandtl number  $Pr = 0.73$ , the amplitude of the wavy surface  $\alpha = 0.2$ , the magnetic parameter  $M = 0.5$ , the Joule heating parameter  $J = 0.01$  and the viscous dissipation parameter  $Ec = 0.02$ . The increasing value of  $Q$  generates more heat within the boundary layer which increase temperature. Increasing heat increases velocity which is clearly shown in figure 3.1(a). It is seen that the velocity increases approximately 33.08 % for same value of  $\eta = 1.36929$  when  $Q$  increases from 0.30 to 1.00. ( Lowest at  $x = 1.36929, y = 0.61415$ ; Highest at  $x = 1.36929, y = 0.77074$  )

Figure 3.2(a) and (b) deal with the effect of different values of Joule heating parameter  $J = (0.001, 0.009, 0.020, 0.040)$  on the velocity profile  $f'(x,\eta)$  and the temperature profile  $\theta(x,\eta)$  with Prandtl number  $Pr = 0.73$ , the amplitude of the wavy surface  $\alpha = 0.2$ , the heat generation parameter  $Q = 0.30$ , the viscous dissipation parameter  $Ec = 0.02$ . Although the effects of Joule heating can not be seen well in the graph for velocity and temperature, the variation can be found in value comparism. In figure 3.2(a), the velocity profiles increase 0.11% for same value of  $\eta = 1.3024$  when  $J$  increases from 0.001 to 0.040. Joule heating produce heat in the flow therefore flow temperature increases. At the surface the temperature profile is maximum and decreases away from the surface and finally takes asymptomatic values.

Figure 3.3(a) and (b) deal with the effect of different values of Magnetic parameter  $M = (0.00, 1.00, 2.00, 3.00)$  on the velocity profile  $f'(x,\eta)$  and the temperature profile  $\theta(x,\eta)$  with Prandtl number  $Pr = 0.73$ , the amplitude of the wavy surface  $\alpha = 0.2$ , the heat generation parameter  $Q = 0.3$ , the viscous dissipation parameter  $Ec = 0.02$ . In figure 3.3(a), the velocity profile decrease 43.81% for difeerent values of  $\eta$  upto the position  $\eta = 4.0$  as  $M$  increases from 0.0 to 3.0, after that position the velocity profile increase with the increase of magnetic parameter  $M$ . For natural convection flow, the velocity profiles shows different values along  $\eta$  direction i.e., the velocity is zero at the boundary wall then the velocity reach

to the peak value as  $\eta$  increases and finally the velocity approaches to the asymptotic value (zero). The velocity profiles having higher peak values for lower values of magnetic parameter tends to decrease comparatively faster along  $\eta$  direction than velocity profiles having lower peak values for higher values of magnetic parameter. So all the velocity profiles meet together at the position of  $\eta = 4.0$  and cross the side. Heat produces due to the interaction between Joule heating and adjacent magnetic field, consequently temperature within the thermal boundary layer increases for increasing values of Joule heating parameter  $J$ . In figure 3.3 (b), it is seen that the temperature profiles is maximum near the surface and decreases away from the surface and finally tends to zero.

In Figure 3.4(a) and (b), It is observed that both the velocity and temperature profile increase slightly for increasing values of viscous dissipation parameter  $Ec = (0.50, 2.00, 3.50, 5.00)$  when the heat generation parameter  $Q = 0.30$ , the Prandtl number  $Pr = 0.73$ , the amplitude of the wavy surface  $\alpha = 0.2$ , the magnetic parameter  $M = 0.02$  and the Joule heating parameter  $J = 0.01$ . It is expected because increasing value of  $N$  increases thermal energy inside the boundary layer due to fluid friction which is obviously increase convection and ultimately increase velocity. In the viscous dissipation process heat is automatically generated which increases temperature of the fluid flow. It is noted that velocity increases 5.12 % for the same value of  $\eta$  as  $Ec$  increases from 0.50 to 5.00. (Lowest at  $x=1.36929, y=0.61415$ ; Highest at  $x=1.36929, y=0.64727$ )

Figure 3.5 (a) demonstrates the velocity profiles for variation of Prandtl number  $Pr = (0.73, 1.74, 3.00, 7.00)$  while heat generation parameter  $Q = 0.30$ , the amplitude of the wavy surface  $\alpha = 0.20$ , the magnetic parameter  $M = 0.01$ , Joule heating parameter  $J = 0.04$  and the viscous dissipation parameter  $Ec = 0.02$  and the corresponding temperature profile is shown in figure 3.5 (b). It is well known that Prandtl number is the ratio of viscous force and thermal force. So, increasing values of  $Pr$  increase viscosity and decrease thermal action of the fluid. If viscosity increase, then fluid does not move freely. Because of this fact, it can be observed from figure 3.5 (a) that the velocity of the fluid decreases with the increasing value of Prandtl number  $Pr$ . The figure shows that the velocity decreases 49.10% for different values of  $\eta$  due to the increased values of  $Pr$ . Since the thermal force decreases, so the temperature decreases significantly with increasing values of  $Pr$ .

The variation of the velocity profile and the temperature profile for different values of amplitude of the wavy surface  $\alpha = (0.0, 0.1, 0.2, 0.3)$  in case of the Prandtl number  $Pr = 0.73$ , the heat generation parameter  $Q = 0.3$ , the magnetic parameter  $M = 0.01$ , Joule heating parameter  $J=0.04$  and the viscous dissipation parameter  $Ec = 0.02$  are shown in figure 3.6 (a) and (b). Figure 3.6 (a) shows the small increment on the velocity  $f' (x,\eta)$  for increasing values of  $\alpha$ . It is seen that the velocity increases 3.82 % for different values of  $\eta$  when  $\alpha$  increases from 0.0 to 0.3. Figure 3.6(b) depicts the temperature profile  $\theta(x,\eta)$ , which increases slowly with the increase of the amplitude of wavy surface.

### **Skin Friction Coefficient and Rate of Heat Transfer**

The influence of the parameter  $Q$ , on the skin friction coefficient  $C_{fx}$  and local rate of heat transfer  $Nu_x$  are illustrated in Figures 3.7(a) and (b) respectively while  $\alpha = 0.2$ ,  $Ec = 0.02$ ,  $M = 0.5$ ,  $J=0.02$  and  $Pr = 0.73$ . From those it is observed that an increase in the heat generation parameter  $Q = (0.30, 0.50, 0.70, 1.0)$  leads to increase the local skin friction coefficient  $C_{fx}$  and decrease the local rate of heat transfer  $Nu_x$  at different position of  $x$ . These happen, since the heat generation mechanism creates a layer of hot fluid near the surface and finally the resultant temperature of the fluid exceed the surface temperature and temperature gradient decreases. For this reason the rate of heat transfer decreases. Increasing temperature increases the viscosity of the fluid. Hence the corresponding shearing stress in terms of local skin friction coefficient increases. It is seen that the local skin friction coefficient  $C_{fx}$  increases 57.21 % for different values of  $x$  when  $Q$  increases from 0.30 to 1.00.

The variation of local skin friction  $C_{fx}$  and the rate of heat transfer in terms of the local Nusselt number  $Nu_x$  for the Joule heating parameter  $J = (0.001, 0.009, 0.020, 0.040)$  against  $x$  from the wavy surface while  $\alpha = 0.2$ ,  $Q = 0.3$ ,  $M = 0.01$ ,  $Ec = 0.02$  and  $Pr = 0.73$  are illustrated in figure 3.8(a) and (b) respectively. The higher value of  $J$  accelerates the fluid flow and increases the temperature, So from the figure it is noted that for the Joule heating parameter  $J$ , the skin friction coefficient increases along the upstream direction of the surface and to decrease of the heat transfer rates. It is seen that the local skin friction coefficient  $C_{fx}$  increases 8.56 % for same values of  $x = 9.50$  when  $J$  increases from 0.001 to 0.040.

In figures 3.9(a) and (b), the skin friction coefficient  $C_{fx}$  and local rate of heat transfer  $Nu_x$  are illustrated for different values of  $M$  while  $J = 0.01$ ,  $\alpha = 0.2$ ,  $Ec = 0.02$ ,  $Q = 0.3$  and  $Pr = 0.73$ . Here it is observed that an increase in the magnetic parameter  $M = (0.00, 1.00, 2.00, 3.00)$  leads to decrease the local skin friction coefficient and local rate of heat transfer at different position of  $x$ . The magnetic field acts against the flow and reduces the skin friction and the rate of heat transfer. It is seen that the local skin friction coefficient  $C_{fx}$  decreases 50.06 % for different values of  $x$  when  $M$  increases from 0.0 to 3.0

The variation of local skin friction  $C_{fx}$  and the rate of heat transfer in terms of the local Nusselt number  $Nu_x$  for the viscous dissipation parameter  $Ec = (0.50, 2.00, 3.50, 5.00)$  against  $x$  from the wavy surface while  $\alpha = 0.2$ ,  $Q = 0.3$ ,  $M = 0.02$ ,  $J = 0.01$  and  $Pr = 0.73$  are illustrated in figure 3.10(a) and (b) respectively. Increasing value of  $Ec$  accelerates the fluid flow and increases the temperature. Accordingly, from the figure it is noted that for the viscous dissipation parameter  $Ec$ , the skin friction coefficient increases along the upstream direction of the surface and to decrease of the heat transfer rates. It is seen that the local skin friction coefficient  $C_{fx}$  increases 83.83 % for same values of  $x = 9.50$  when  $N$  increases from 0.50 to 5.00.

Figures 3.11 (a) and (b) show the local skin friction  $C_{fx}$  and the rate of heat transfer in terms of the local Nusselt number  $Nu_x$  for different values of Prandtl number  $Pr = (0.73, 1.74, 3.00, 7.00)$  when amplitude of wavy surface  $\alpha = 0.20$ , the heat generation parameter  $Q = 0.30$ , the magnetic parameter  $M = 0.01$ ,  $J = 0.04$  and the viscous dissipation parameter  $Ec = 0.02$ . It is observed from figure 3.11(a) that the increasing values of Prandtl number  $Pr$  leads to decrease monotonically the skin friction coefficient and opposite result is observed on the rate of heat transfer in figure 3.11(b). Increasing the values of Prandtl number  $Pr$  speed up the decay of the temperature field away from the heated surface with a consequent increase in the rate of heat transfer and a reduction in the thermal boundary layer thickness.

In figures 3.12 (a) and 3.12 (b), the surface shear stress in terms of the local skin friction  $C_{fx}$  and the rate of heat transfer in terms of the local Nusselt number  $Nu_x$  are depicted graphically for the different values of amplitude of wavy surface  $\alpha = (0.0, 0.1, 0.2, 0.3)$  when the value of Prandtl number  $Pr = 0.73$ , the heat generation parameter  $Q = 0.3$ , the magnetic parameter  $M = 0.01$ , the Joule heating parameter  $J = 0.04$  and the viscous dissipation parameter  $Ec =$

0.02. Since the velocity force decreases at local points due to increasing the surface waviness, so the figures depicts that increase in the value of amplitude of wavy surface  $\alpha$  tends to decrease the value of skin friction coefficient  $C_{fx}$  and the rate of heat transfer in terms of the local Nusselt number  $Nu_x$ . It is seen that the local skin friction coefficient  $C_{fx}$  increases 0.66 % for different values of  $x$  when  $\alpha$  increases from 0.0 to 0.3.

### **Streamlines and Isotherms:**

Figure 3.13 and 3.14 illustrate the effect of variation of the  $Q$  equal to 0.30, 0.50, 0.70 and 1.0 on the streamlines and isotherms respectively while  $\alpha = 0.2$ ,  $Ec = 0.02$ ,  $M = 0.5$ ,  $J = 0.01$  and  $Pr = 0.73$ . Figure 3.13 depicts that the maximum values of  $\psi$  increases while the values of  $Q$  increases that is the values of  $\psi_{max}$  are 14.67, 17.55, 20.37 and 24.14 for  $Q = 0.30, 0.50, 0.70$  and 1.0 respectively. It is noted from figure 3.14 that as the value of  $Q$  increases the thermal boundary layer becomes thicker gradually. So the isotherms increase while the values of  $Q$  increase.

In a fixed value of  $\alpha = 0.2$ ,  $Ec = 0.02$ ,  $M = 0.01$  and  $Pr = 0.73$ , the effect of variation of the  $J$  equal to 0.001, 0.009, 0.020 and 0.040 on the streamlines and isotherms are illustrated by Figure 3.15 and 3.16 respectively. Figure 3.15 depicts that the maximum values of  $\psi$  increases while the values of  $J$  increases that is  $\psi_{max}$  are 13.46, 13.66, 13.85 and 14.00 for  $J = 0.001, 0.009, 0.020$  and 0.040 respectively. From figure 3.16 it is observed that as the value of  $J$  increases the thermal boundary layer becomes thicker gradually. So the increasing values of  $J$  causes the isotherms increasing.

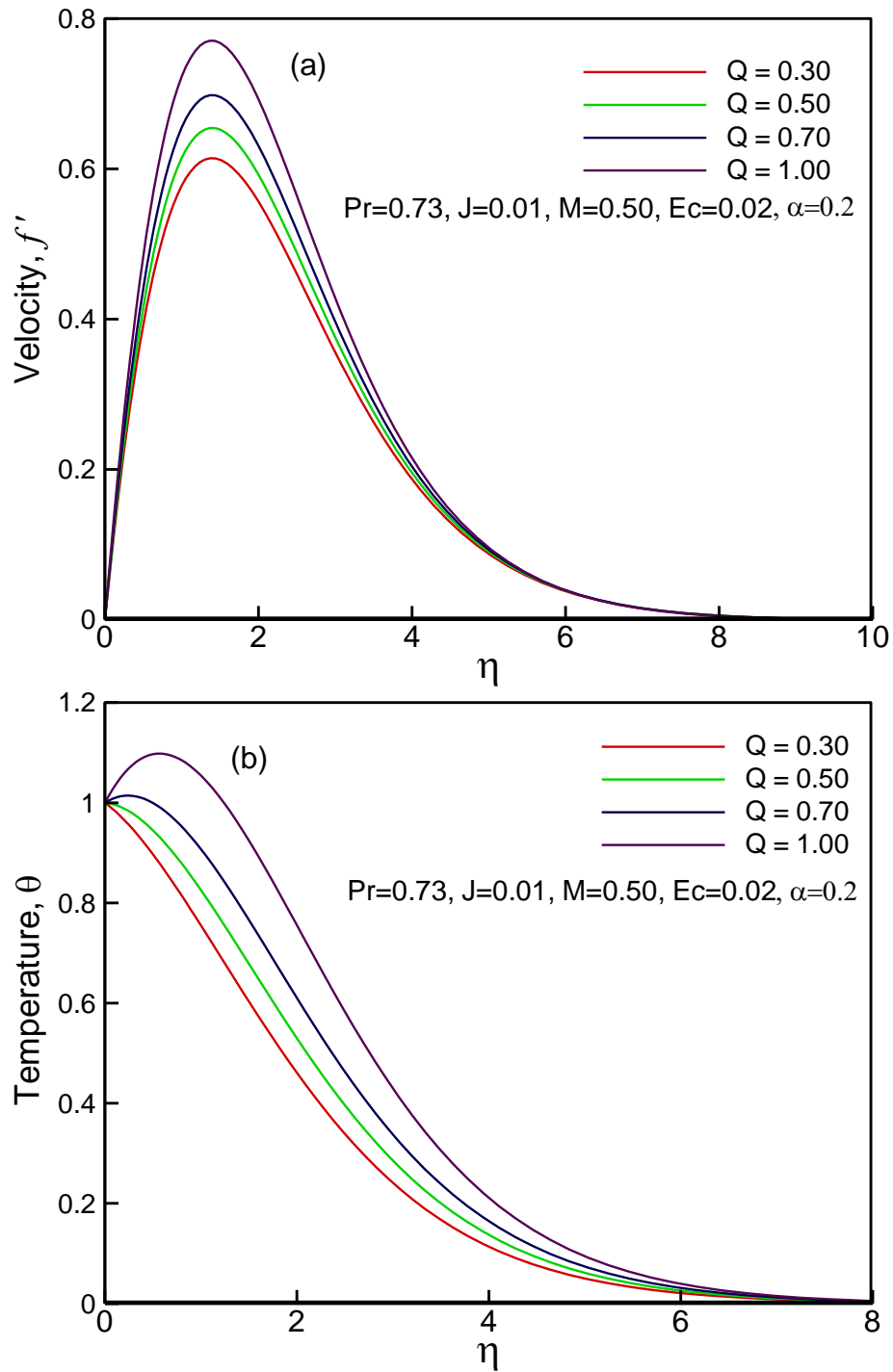
The effect of variation of the surface roughness on the streamlines and isotherms for the values of  $M$  equal to 0.0, 1.0, 2.0, and 3.0 are depicted by figure 3.17 and figure 3.18 while  $Pr = 0.73$ ,  $\alpha = 0.2$ ,  $Q = 0.3$  and  $Ec = 0.02$ . Figure 3.17 depicts that the maximum values of streamline decreases steadily while the values of  $M$  increases. The maximum values of streamlines are 13.50, 12.11, 11.55 and 10.98 for  $M = (0.0, 1.0, 2.0, \text{ and } 3.0)$ . It is observed in figure 3.18 that as the values of  $M$  increases the thermal boundary layer thickness becomes lower gradually that means the layer becomes thinner gradually with the increasing values of  $M$ .

Figure 3.19 and figure 3.20 show the effect of viscous dissipation parameter  $Ec = (0.50, 2.00, 3.50, 5.00)$  on the formulation of streamlines and isotherms respectively while  $Pr = 0.73$ ,  $Q = 0.3$ ,  $M = 0.02$ ,  $J = 0.01$  and  $\alpha = 0.2$ . It is found that for  $Ec = 0.50$  the value of  $\psi_{max}$  is 14.65, for  $Ec = 2.00$  the value of  $\psi_{max}$  is 17.02, for  $Ec = 3.50$   $\psi_{max}$  is 20.01 and for  $Ec = 5.00$   $\psi_{max}$  is 23.93. From figure 3.19, it is seen that the effect of viscous dissipation parameter  $Ec$ , the flow rate in the boundary layer increases. From figure 3.20, it is also observed that due to the effect of  $Ec$ , the thermal state of the fluid increases. Finally, the thermal boundary layer becomes thicker.

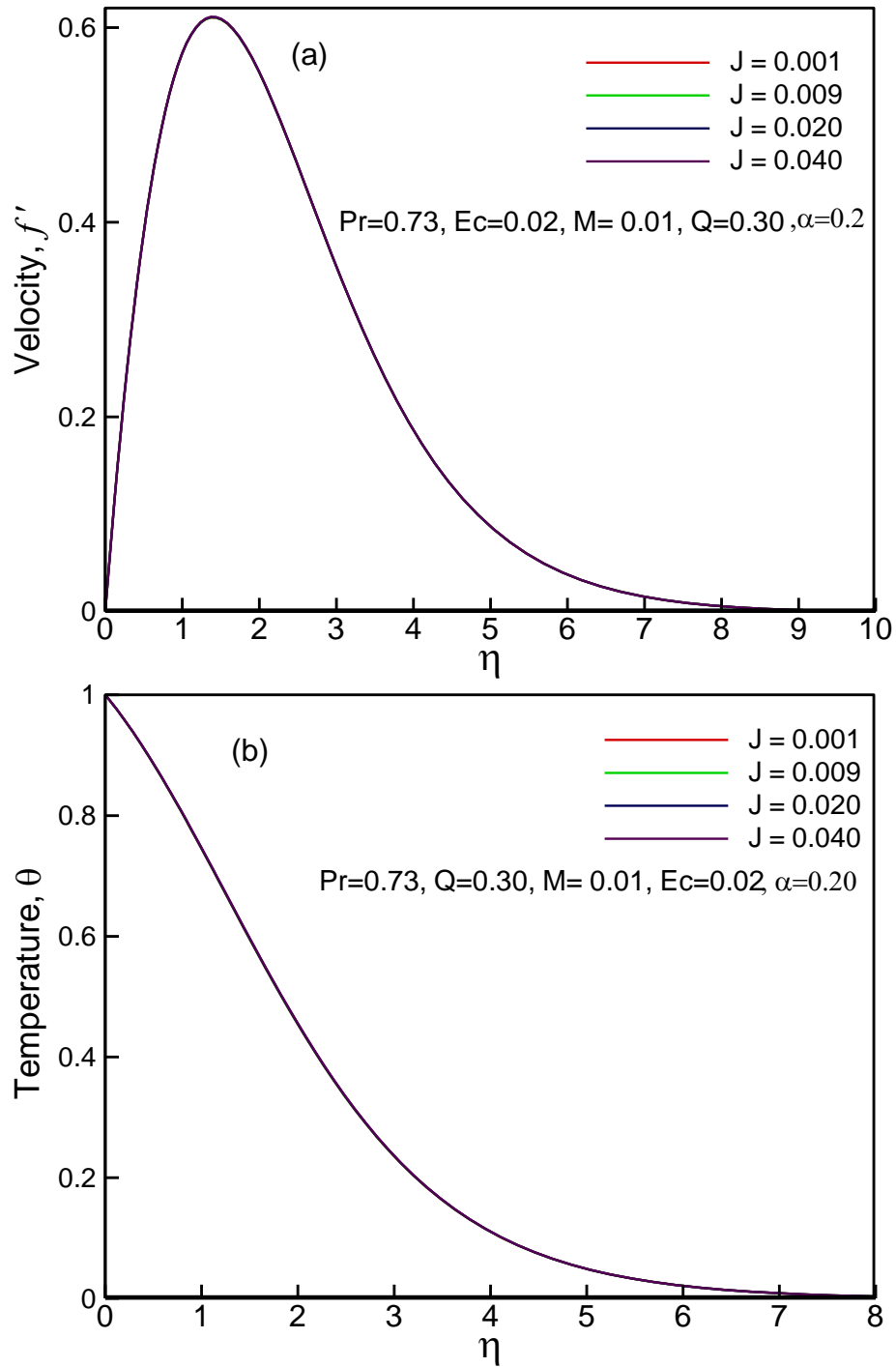
The effect of variation of the surface roughness on the streamlines and isotherms for the values of Prandtl number  $Pr = (0.73, 1.74, 3.00, 7.00)$  are depicted by the figure 3.21 and 3.22 respectively while heat generation parameter  $Q = 0.30$ , amplitude of the wavy surface  $\alpha = 0.20$ , magnetic parameter  $M = 0.01$  and viscous dissipation parameter  $Ec = 0.02$ . It is observed from figure 3.21 that the maximum value of streamlines for  $Pr = 0.73$  is  $\psi_{max} = 13.90$ , for  $Pr = 1.74$  is  $\psi_{max} = 9.93$ , for  $Pr = 3.00$  is  $\psi_{max} = 8.30$  and for  $Pr = 7.00$  is  $\psi_{max} = 6.76$ . So it can be concluded that for increasing values of  $Pr$  with the effect of magnetic parameter and heat generation parameter both the momentum and the thermal boundary layer become thinner.

Figure 3.23 and 3.24 illustrate the velocity boundary layer thickness and thermal boundary layer thickness for the amplitude of the length ratio of the wavy surface  $\alpha = (0.0, 0.1, 0.2, 0.3)$  while heat generation parameter  $Q = 0.3$ , magnetic parameter  $M = 0.01$ , viscous dissipation parameter  $Ec = 0.04$  and Prandtl number  $Pr = 0.73$ . From the figure 3.23 it is observed that the maximum values of streamline are  $\psi_{max} = (13.00, 13.35, 13.65, 14.28)$  for the values of  $\alpha = (0.0, 0.1, 0.2, 0.3)$  respectively. Here it can be concluded that for increasing values of amplitude to the length ratio of the wavy surface  $\alpha$ , the roughness of the wavy surface increases so the velocity boundary layer thickness decreases gradually. Similar result is observed for thermal boundary layer thickness. So isotherms increase for increasing values of amplitude to the length ratio of the wavy surface  $\alpha$ .





**Figure 3.1:** Velocity and temperature profiles for different values of heat generation parameter  $Q$  while  $Pr = 0.73$ ,  $\alpha = 0.2$ ,  $J=0.01$ ,  $Ec = 0.02$ ,  $M = 0.5$



**Figure 3.2:** Velocity and temperature profiles for different values of  $J$  while  $Pr = 0.73$ ,  $\alpha = 0.2$ ,  $Ec = 0.02$ ,  $M = 0.01$   $Q = 0.3$

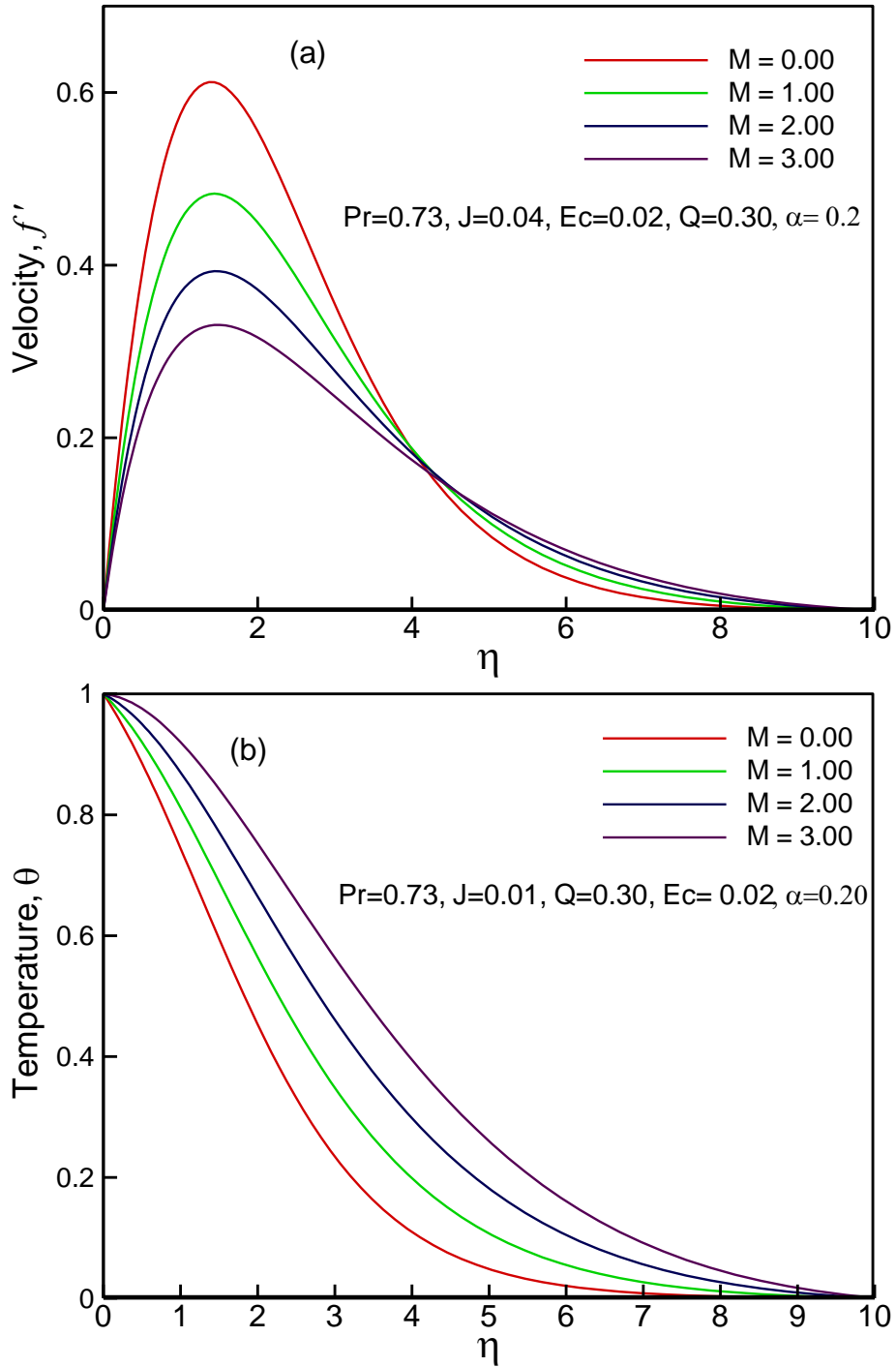


**Figure 3.3:** Velocity and temperature profiles for different values of  $M$  while  $Pr = 0.73, \alpha = 0.2, Ec = 0.02, J = 0.01, Q = 0.3$

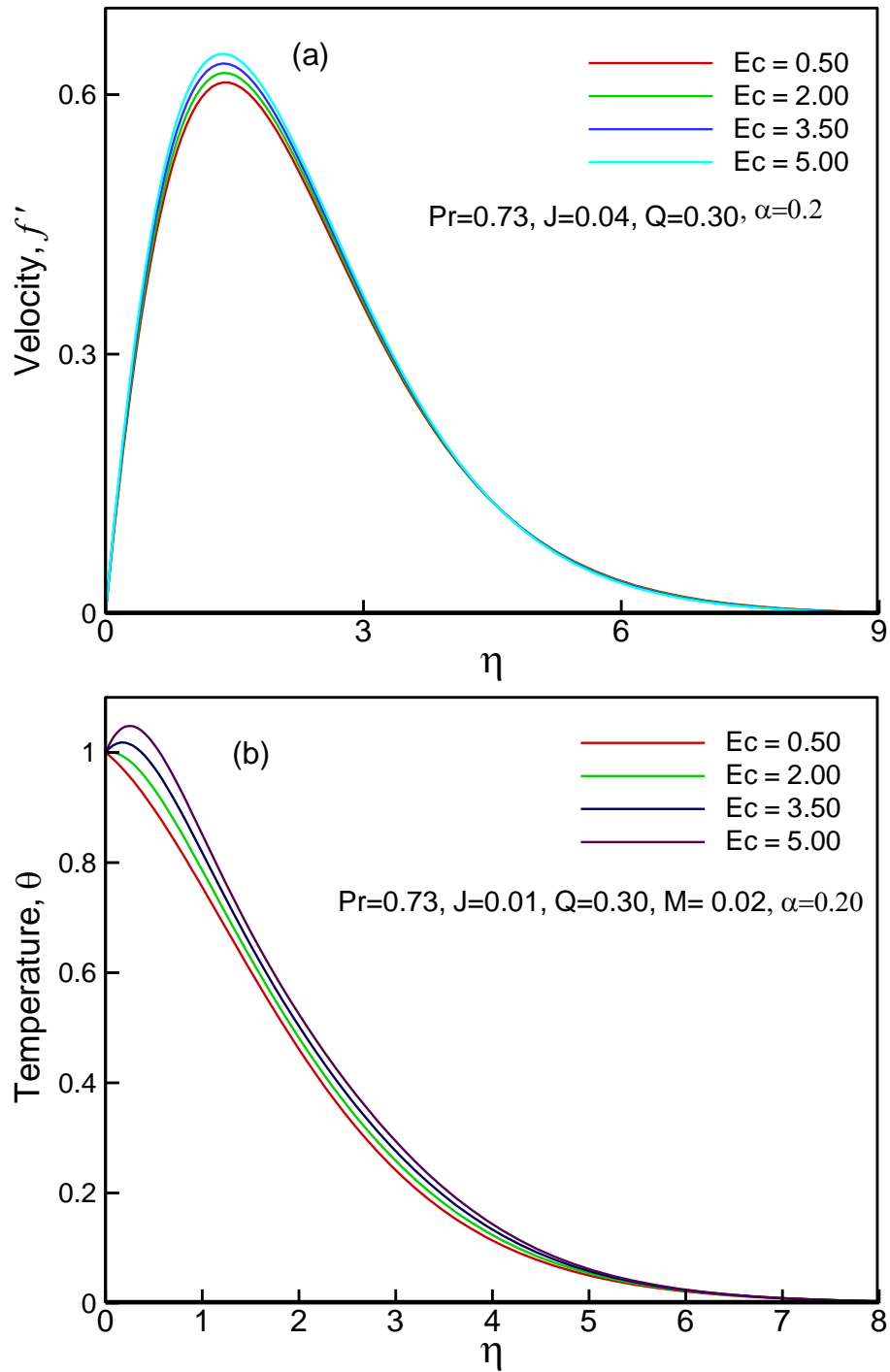


**Figure 3.4:** Velocity and temperature profiles for different values of Viscous dissipation parameter  $Ec$  while  $Pr = 0.73, \alpha = 0.2, J = 0.01, M = 0.02, Q = 0.30$

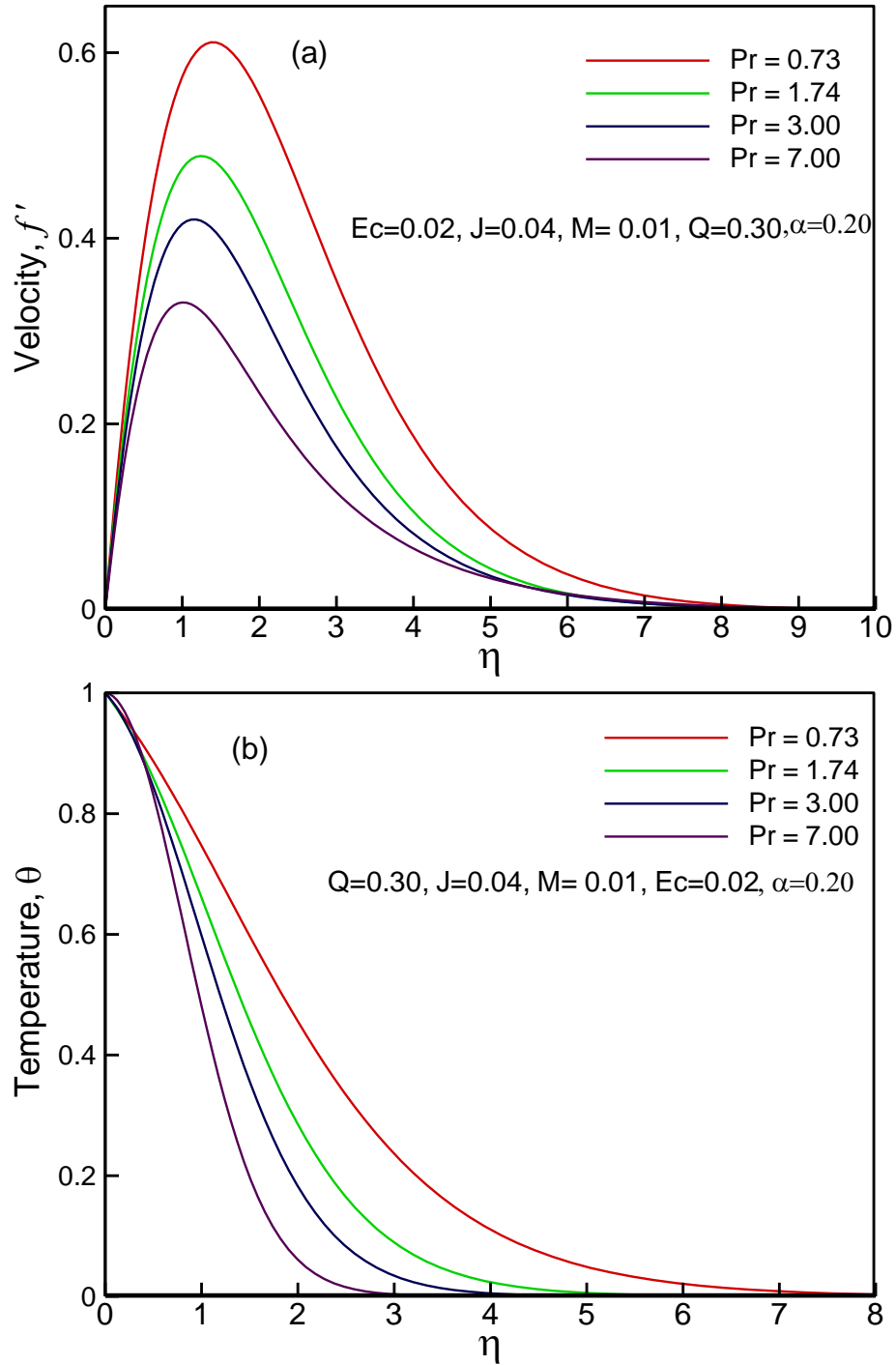


**Figure 3.5:** Velocity and temperature profiles for different values of  $Pr$  while  $J = 0.04, \alpha = 0.2, Ec = 0.02, Q = 0.3, M = 0.01$

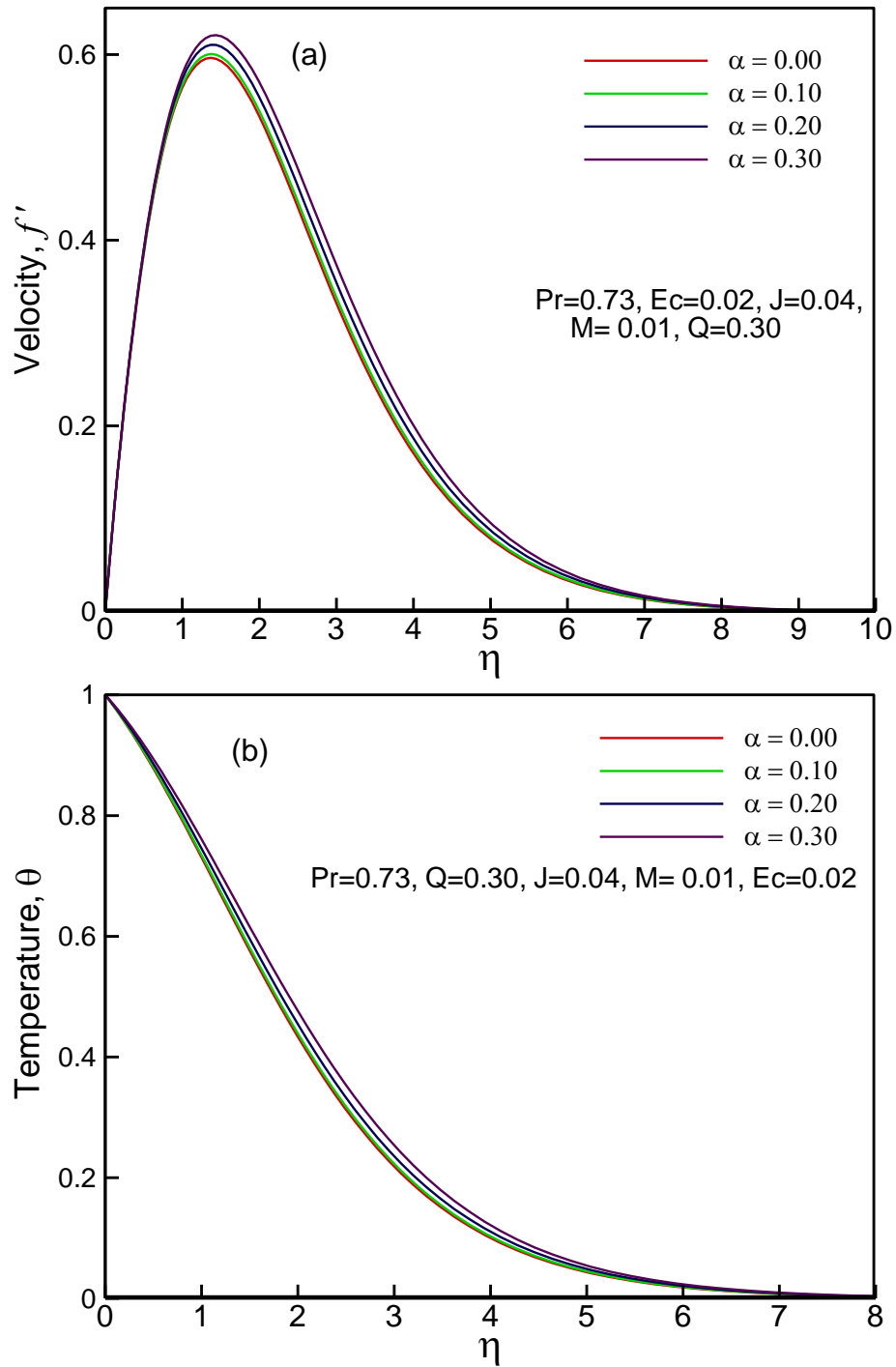


**Figure 3.6:** Velocity and temperature profiles for different values of  $\alpha$  while  $Pr = 0.73, Q = 0.3, J = 0.04, Ec = 0.02, M = 0.01$

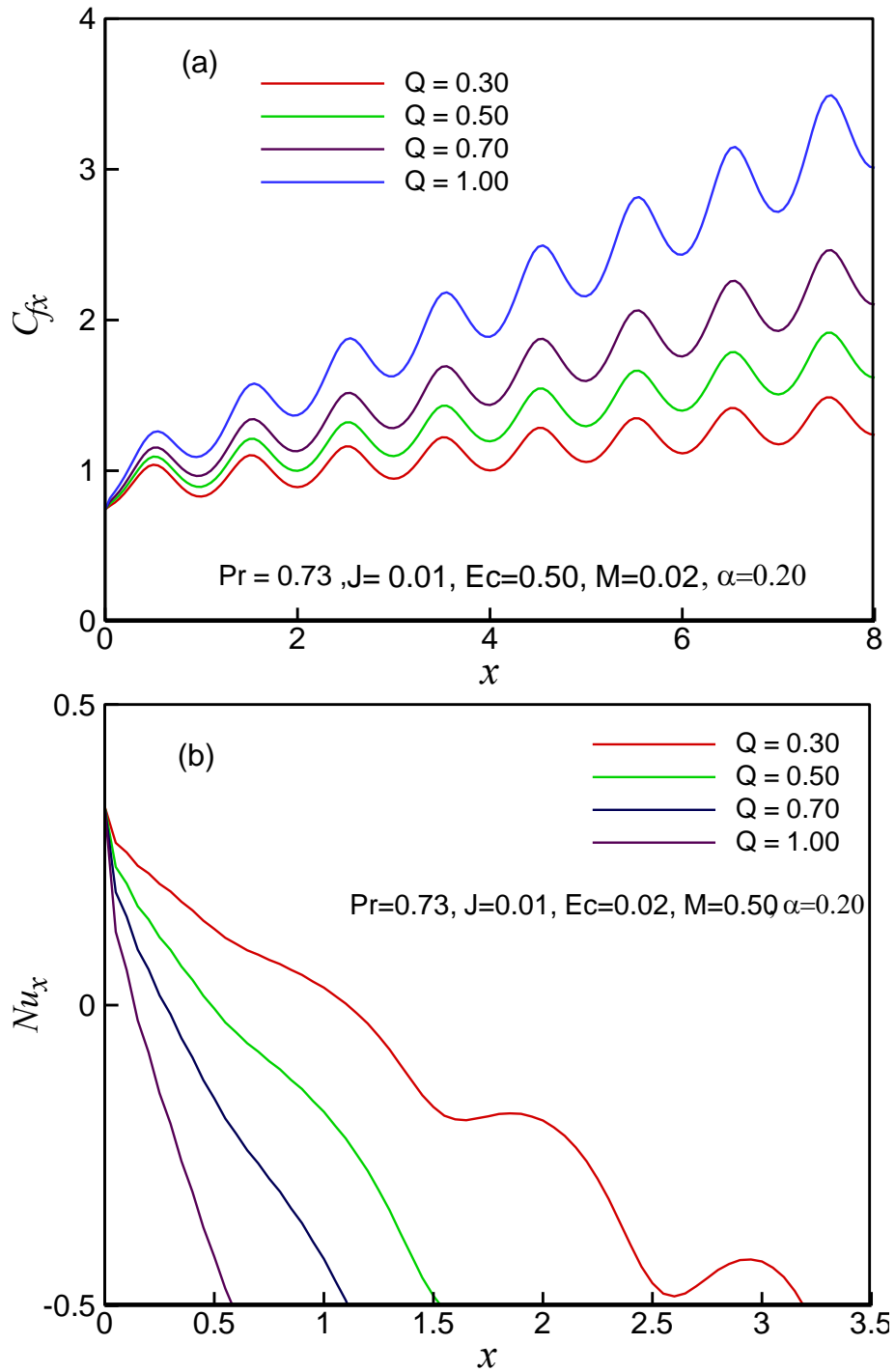


**Figure 3.7:** Skin friction coefficient ( $C_{fx}$ ) and rate of heat transfer ( $Nu_x$ ) for different values of heat generation parameter  $Q$  while  $Pr = 0.73$ ,  $\alpha = 0.2$ ,  $J = 0.01$ ,  $Ec = 0.02$ ,  $M = 0.50$

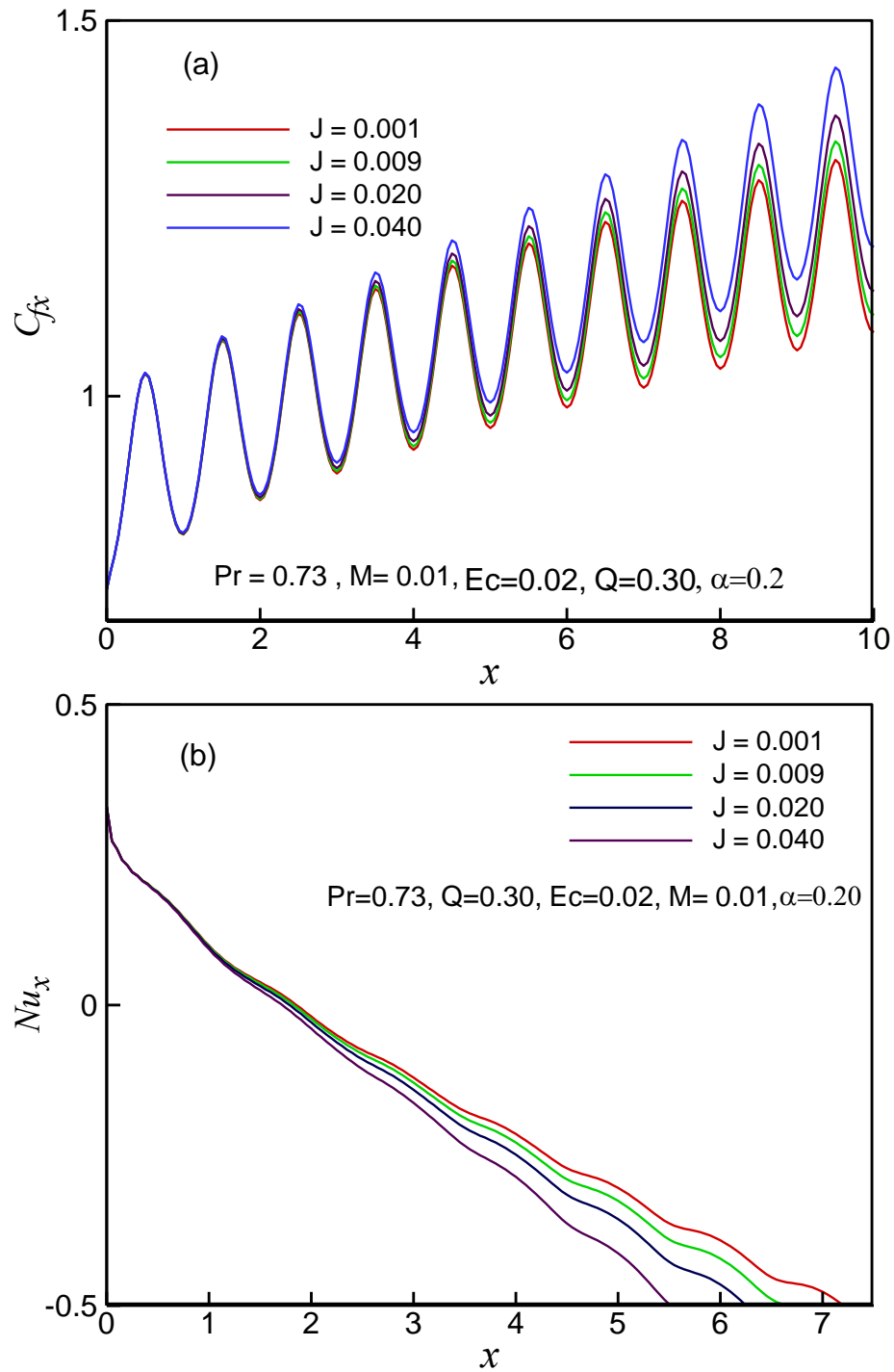


**Figure 3.8:** Skin friction coefficient ( $C_{fx}$ ) and rate of heat transfer ( $Nu_x$ ) for different values of  $J$  while  $Pr = 0.73$ ,  $\alpha = 0.2$ ,  $Ec = 0.02$ ,  $M = 0.01$   $Q = 0.3$



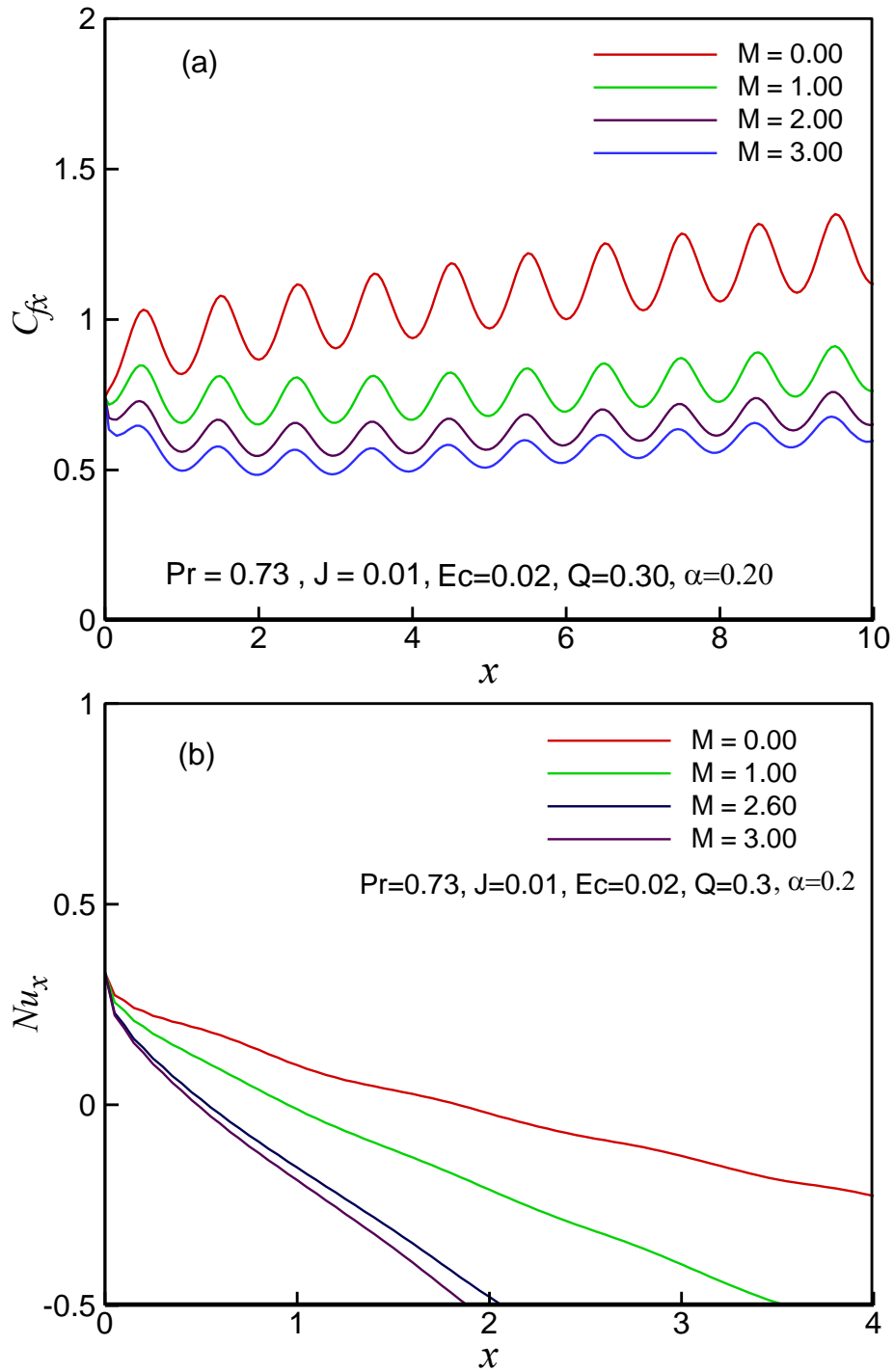


**Figure 3.9:** Skin friction coefficient ( $C_{fx}$ ) and rate of heat transfer ( $Nu_x$ ) for different values of Magnetic parameter  $M$  while  $Pr = 0.73$ ,  $\alpha = 0.2$ ,  $J = 0.01$ ,  $Ec = 0.02$ ,  $Q = 0.30$

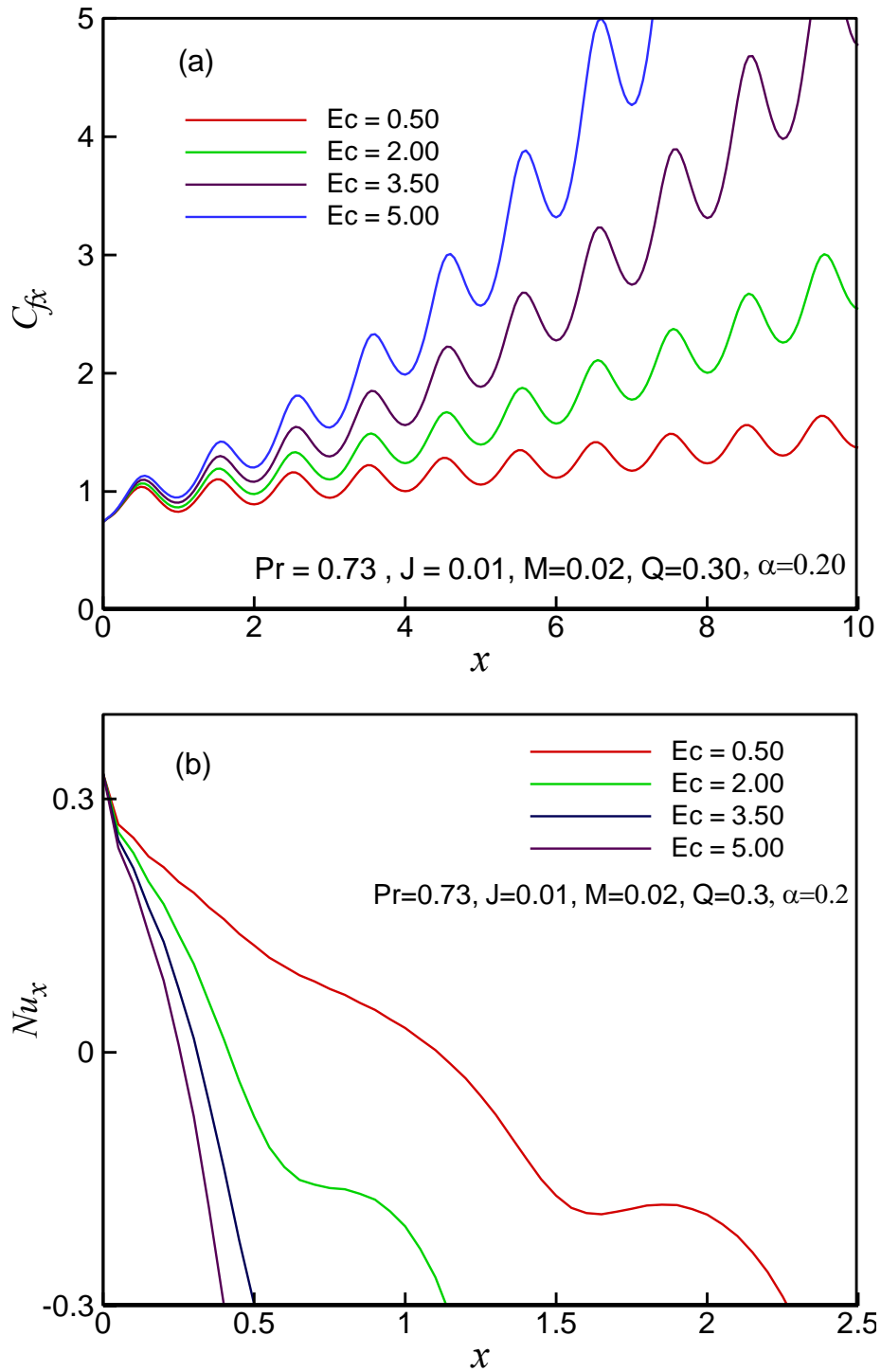


**Figure 3.10:** Skin friction coefficient ( $C_{fx}$ ) and rate of heat transfer ( $Nu_x$ ) for different values of  $Ec$  while  $Pr = 0.73, \alpha = 0.2, J = 0.01, Q = 0.3, M = 0.02$

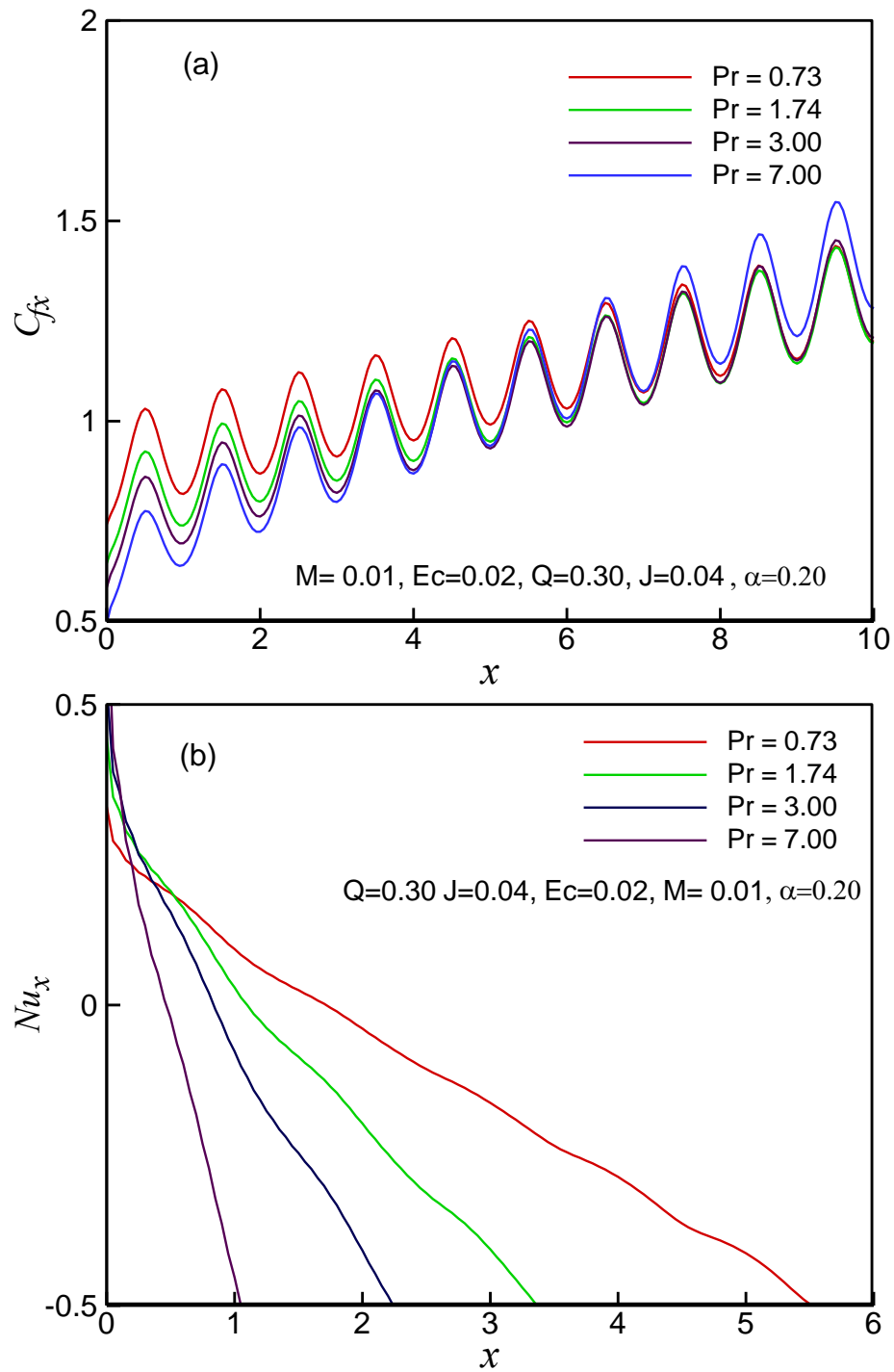


**Figure 3.11:** Skin friction coefficient ( $C_{fx}$ ) and rate of heat transfer ( $Nu_x$ ) for different values of heat generation parameter  $Pr$  while  $Q = 0.30$ ,  $\alpha = 0.20$ ,  $J = 0.04$ ,  $Ec = 0.02$ ,  $M = 0.01$

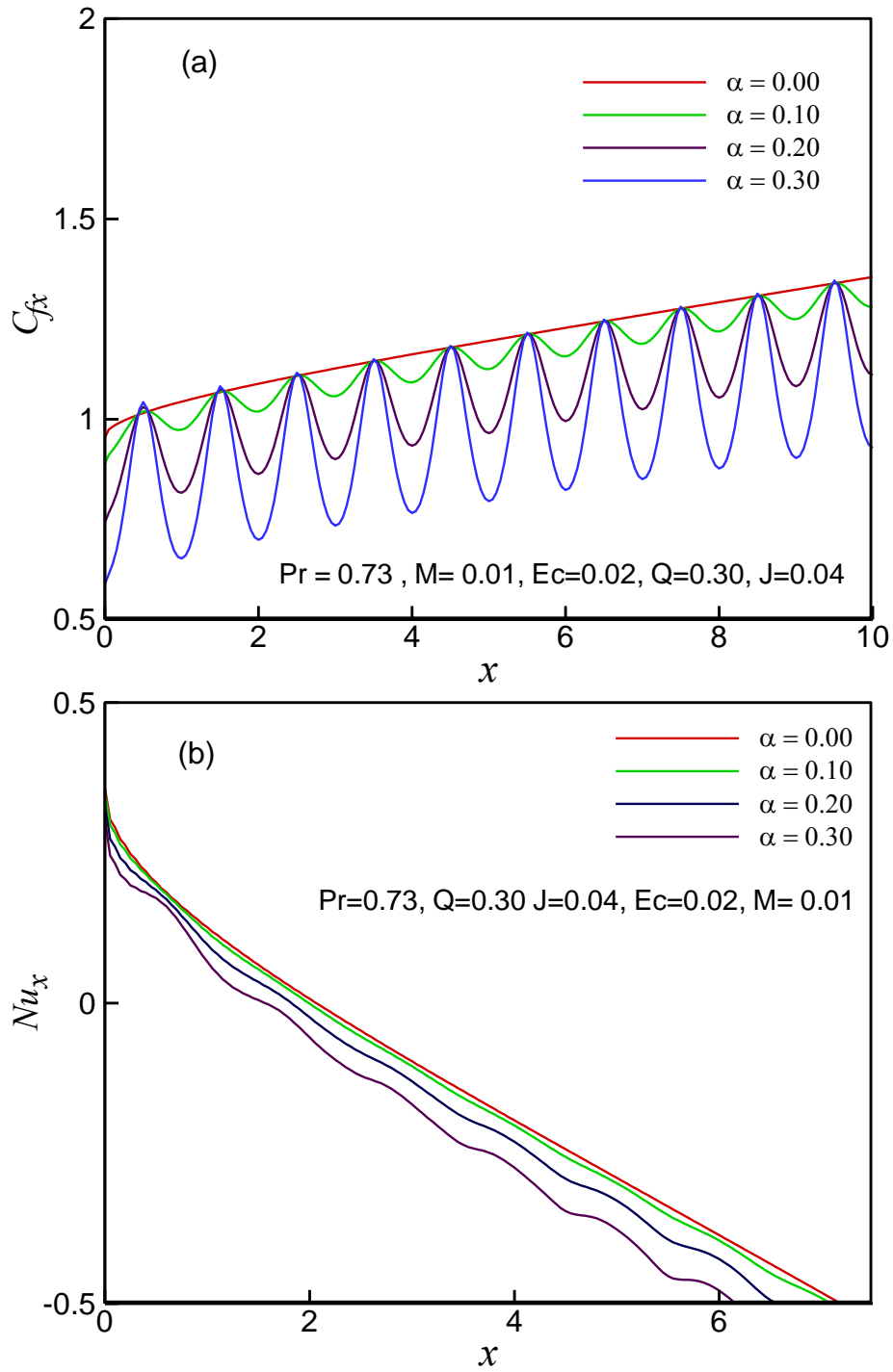


**Figure 3.12:** Skin friction coefficient ( $C_{fx}$ ) and rate of heat transfer ( $Nu_x$ ) for different values of  $\alpha$  while  $Pr = 0.73$ ,  $Q = 0.3$ ,  $J = 0.04$ ,  $Ec = 0.02$ ,  $M = 0.01$

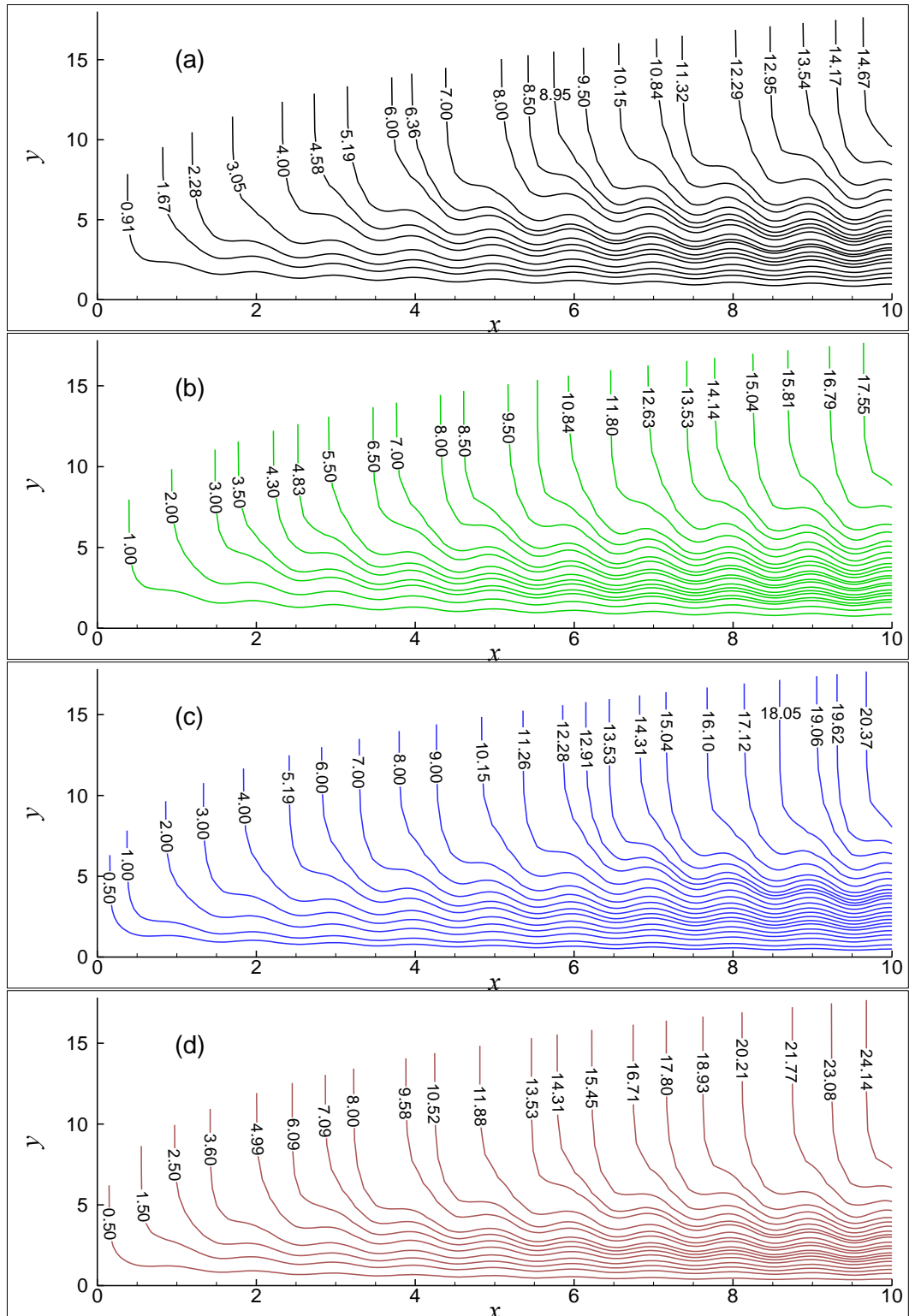


**Figure 3.13:** Streamlines for (a)  $Q = 0.30$ , (b)  $Q = 0.50$ , (c)  $Q = 0.70$  and (d)  $Q = 1.0$  while  $Pr = 0.73$ ,  $\alpha = 0.3$ ,  $J = 0.01$ ,  $Ec = 0.02$ ,  $M = 0.5$

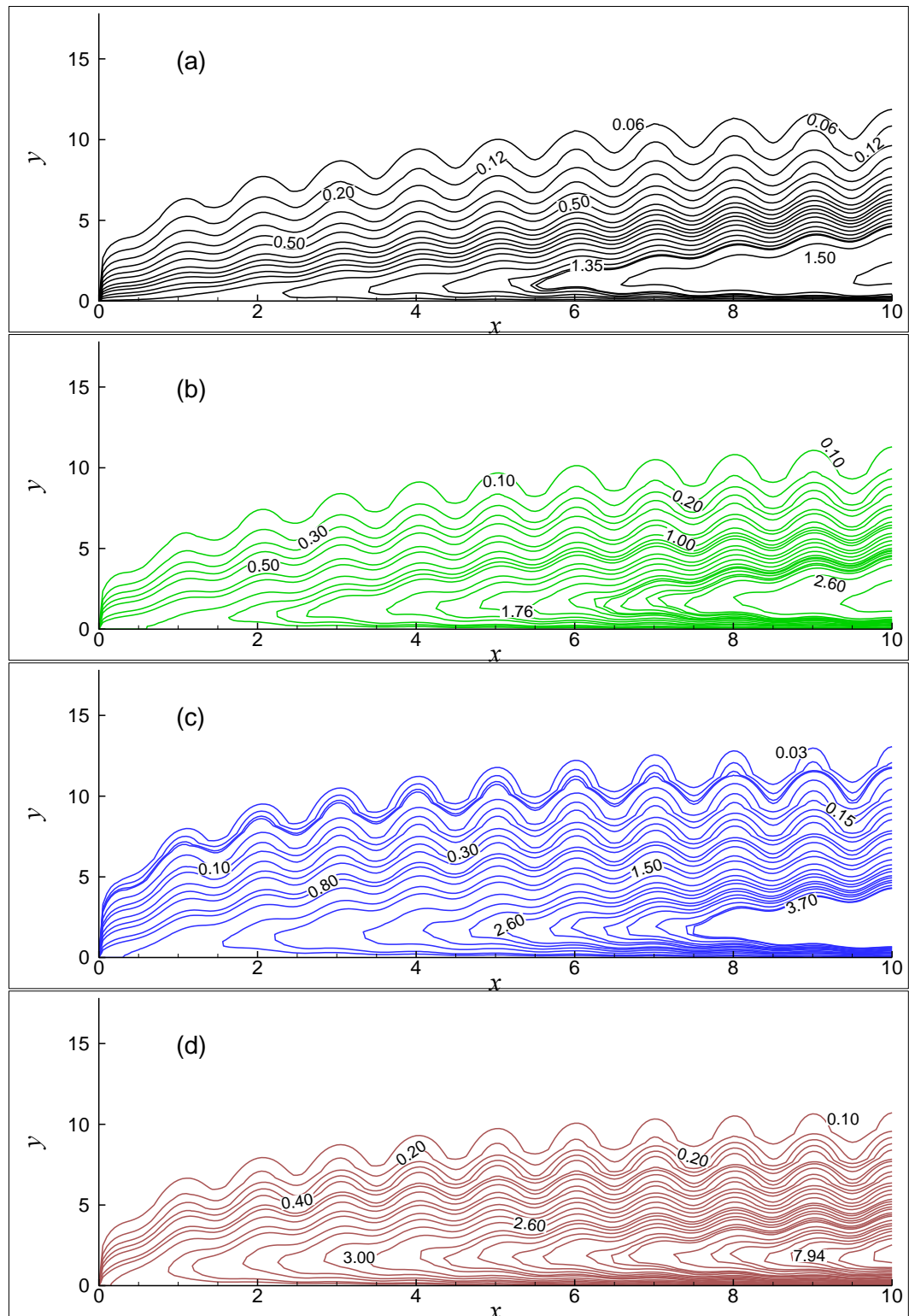


**Figure 3.14:** Isotherms for (a)  $Q = 0.30$ , (b)  $Q = 0.50$ , (c)  $Q = 0.70$  and (d)  $Q = 1.0$  while  $Pr = 0.73$ ,  $\alpha = 0.3$ ,  $J = 0.01$ ,  $Ec = 0.02$ ,  $M = 0.5$

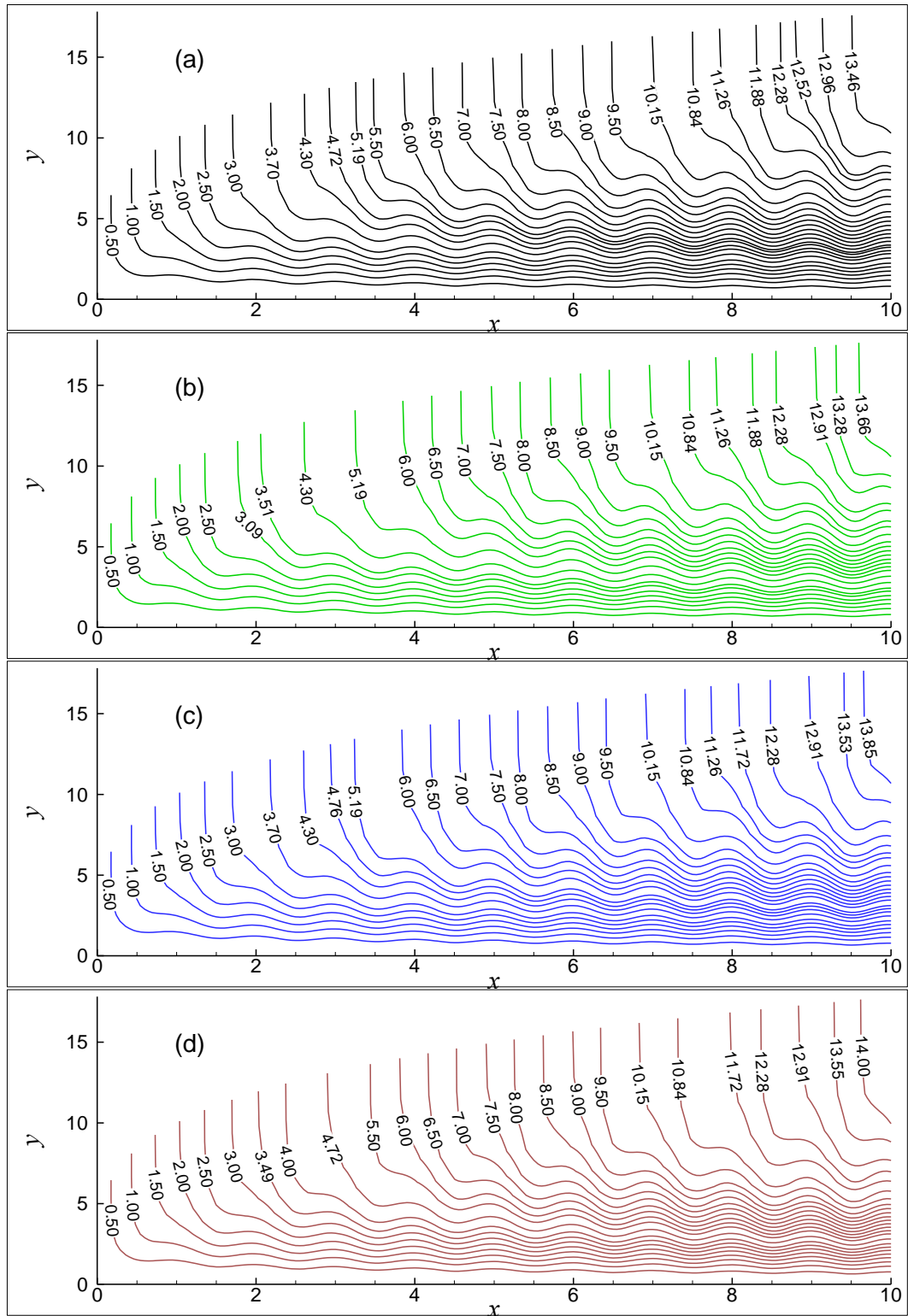


**Figure 3.15:** Streamlines for (a)  $J = 0.001$ , (b)  $J = 0.009$ , (c)  $J = 0.020$  and (d)  $J = 0.040$  while  $Pr = 0.73$ ,  $\alpha = 0.2$ ,  $M = 0.01$ ,  $Ec = 0.02$

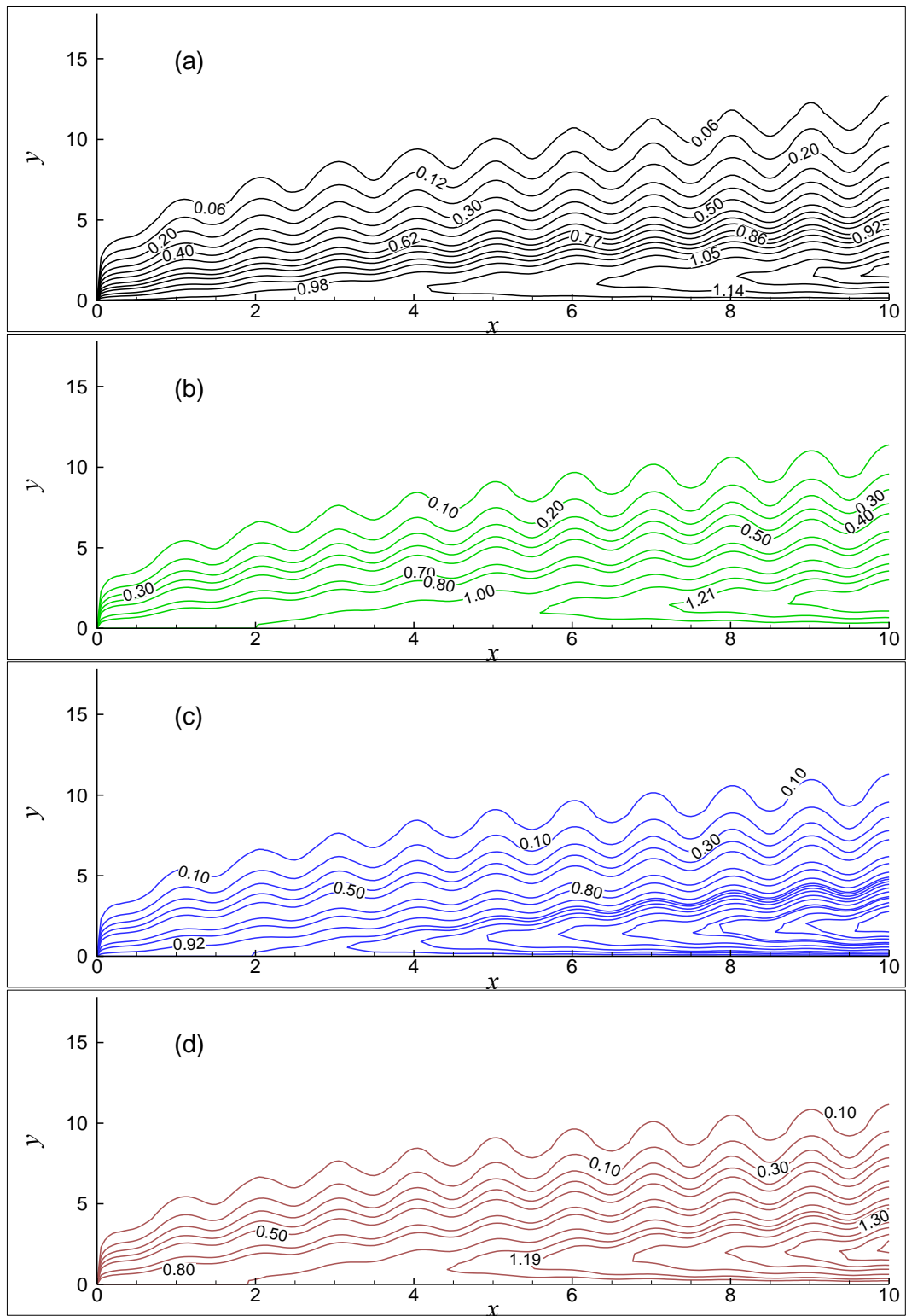


**Figure 3.16:** Isotherms for (a)  $J = 0.001$ , (b)  $J = 0.009$ , (c)  $J = 0.020$  and (d)  $J = 0.040$  while  $Pr = 0.73$ ,  $\alpha = 0.2$ ,  $M = 0.01$ ,  $Ec = 0.02$



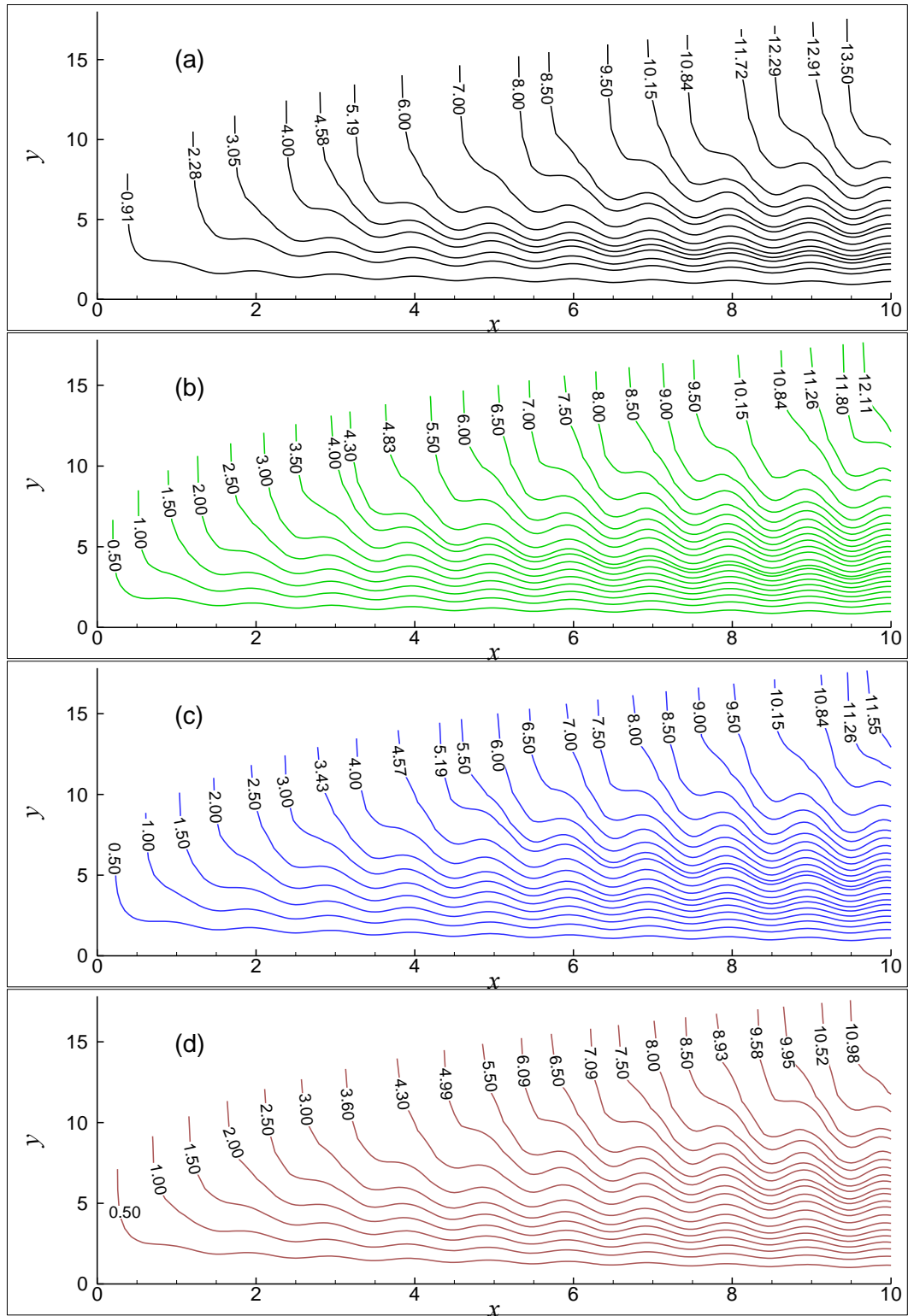


**Figure 3.17:** Streamlines for (a)  $M = 0.0$ , (b)  $M = 1.0$ , (c)  $M = 2.0$  and (d)  $M = 3.0$  while  $Pr = 0.73$ ,  $\alpha = 0.2$ ,  $Ec = 0.02$ ,  $Q = 0.3$

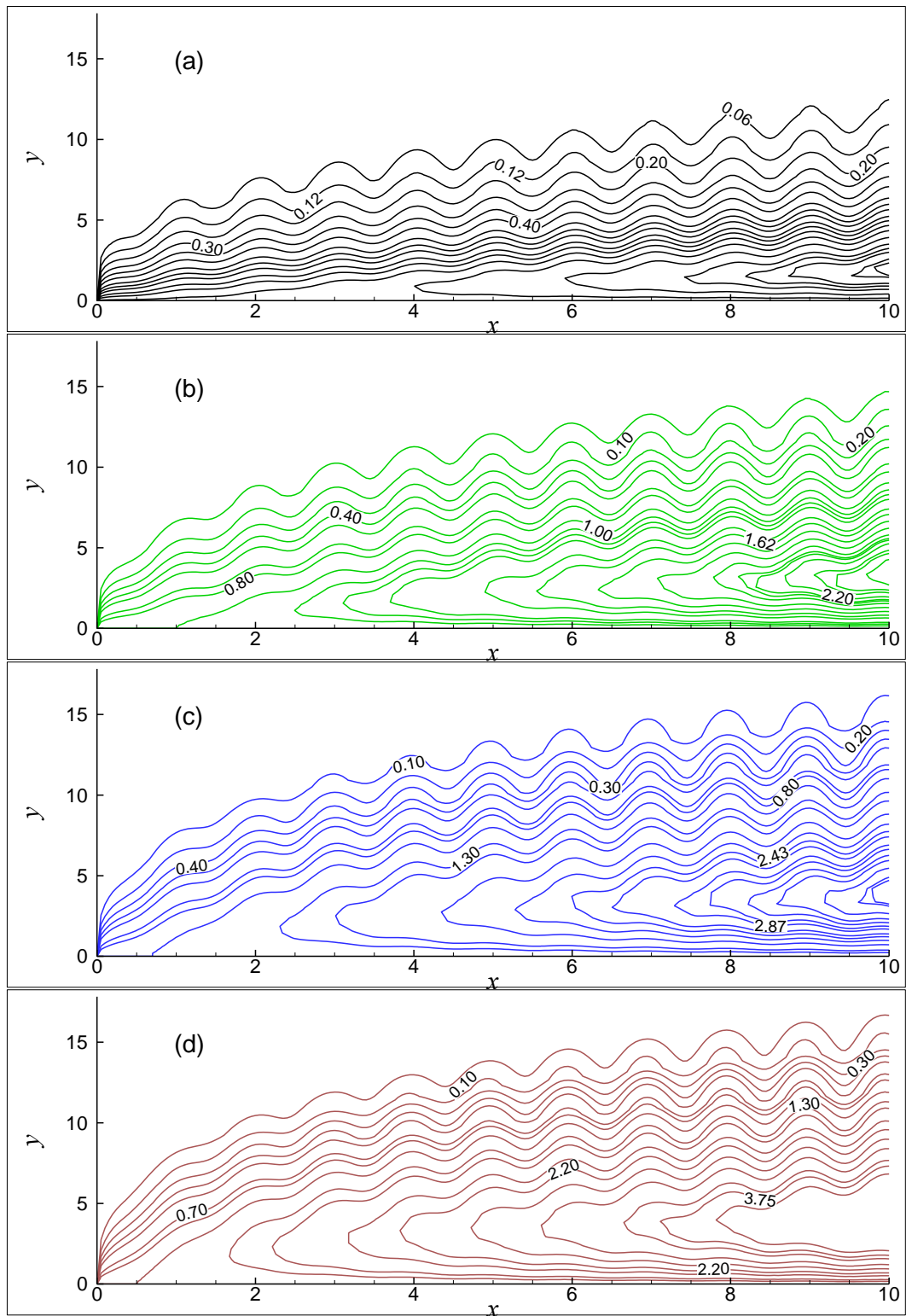


**Figure 3.18:** Isotherms for (a)  $M = 0.0$ , (b)  $M = 1.0$ , (c)  $M = 2.0$  and (d)  $M = 3.0$  while  $Pr = 0.73$ ,  $\alpha = 0.2$ ,  $Ec = 0.02$ ,  $Q = 0.3$

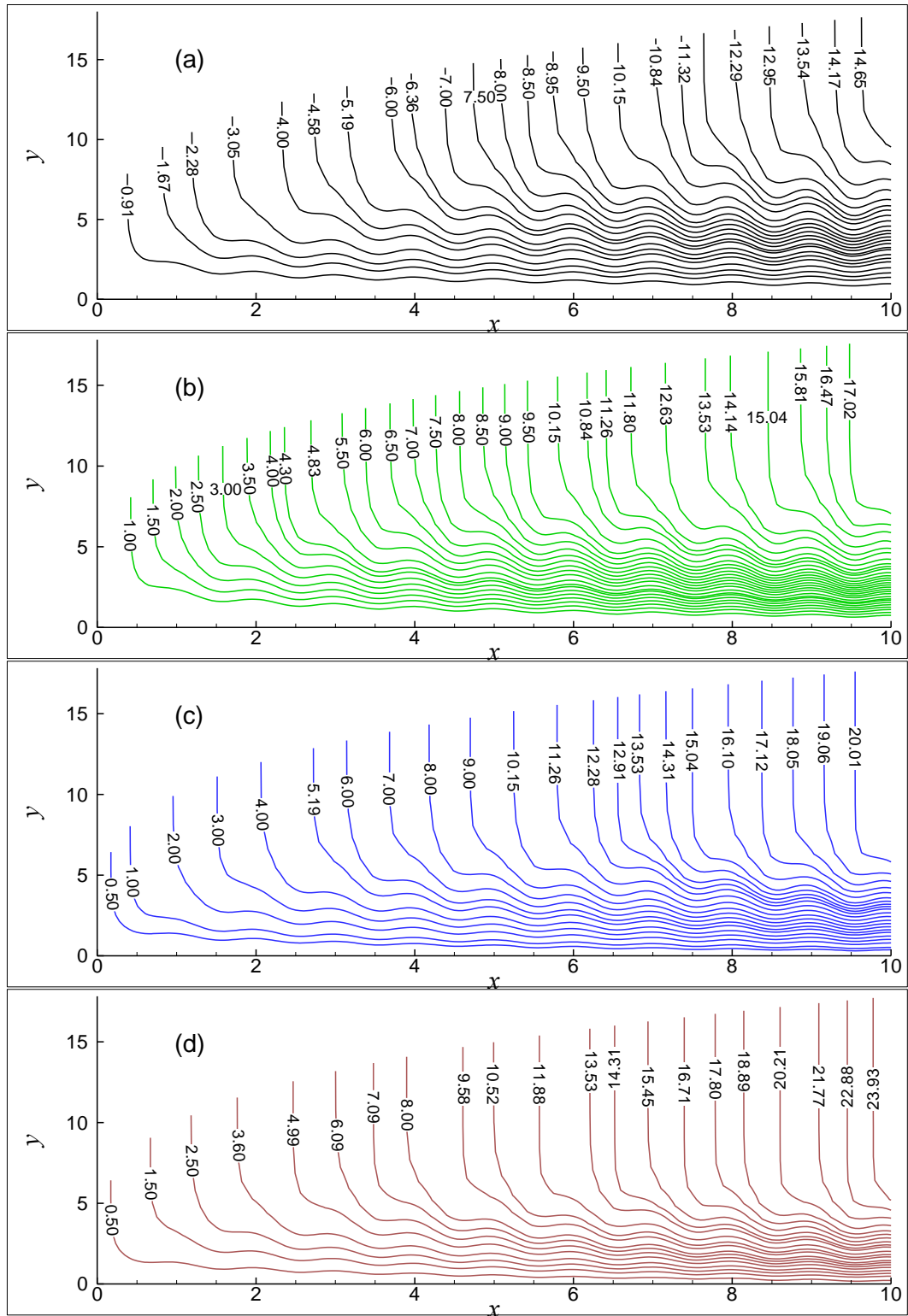


**Figure 3.19:** Streamlines for (a)  $Ec = 0.50$ , (b)  $Ec = 2.00$ , (c)  $Ec = 3.50$  and (d)  $Ec = 5.00$  while  $Pr = 0.73$ ,  $\alpha = 0.2$ ,  $J = 0.01$ ,  $M = 0.02$

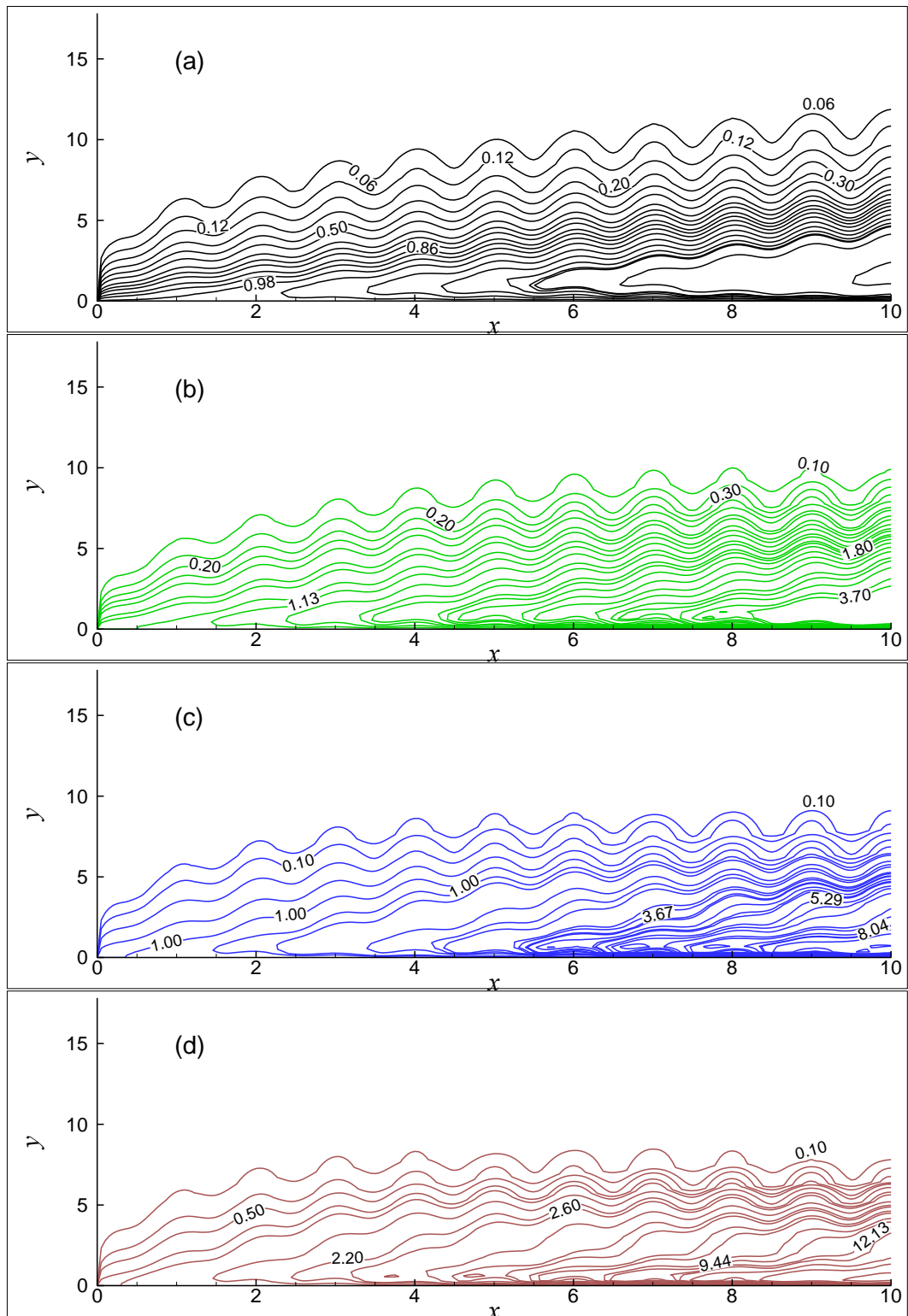


**Figure 3.20:** Isotherms for (a)  $Ec = 0.50$ , (b)  $Ec = 2.00$ , (c)  $Ec = 3.50$  and (d)  $Ec = 5.00$  while  $Pr = 0.73$ ,  $\alpha = 0.2$ ,  $J = 0.01$ ,  $Q = 0.3$ ,  $M = 0.02$

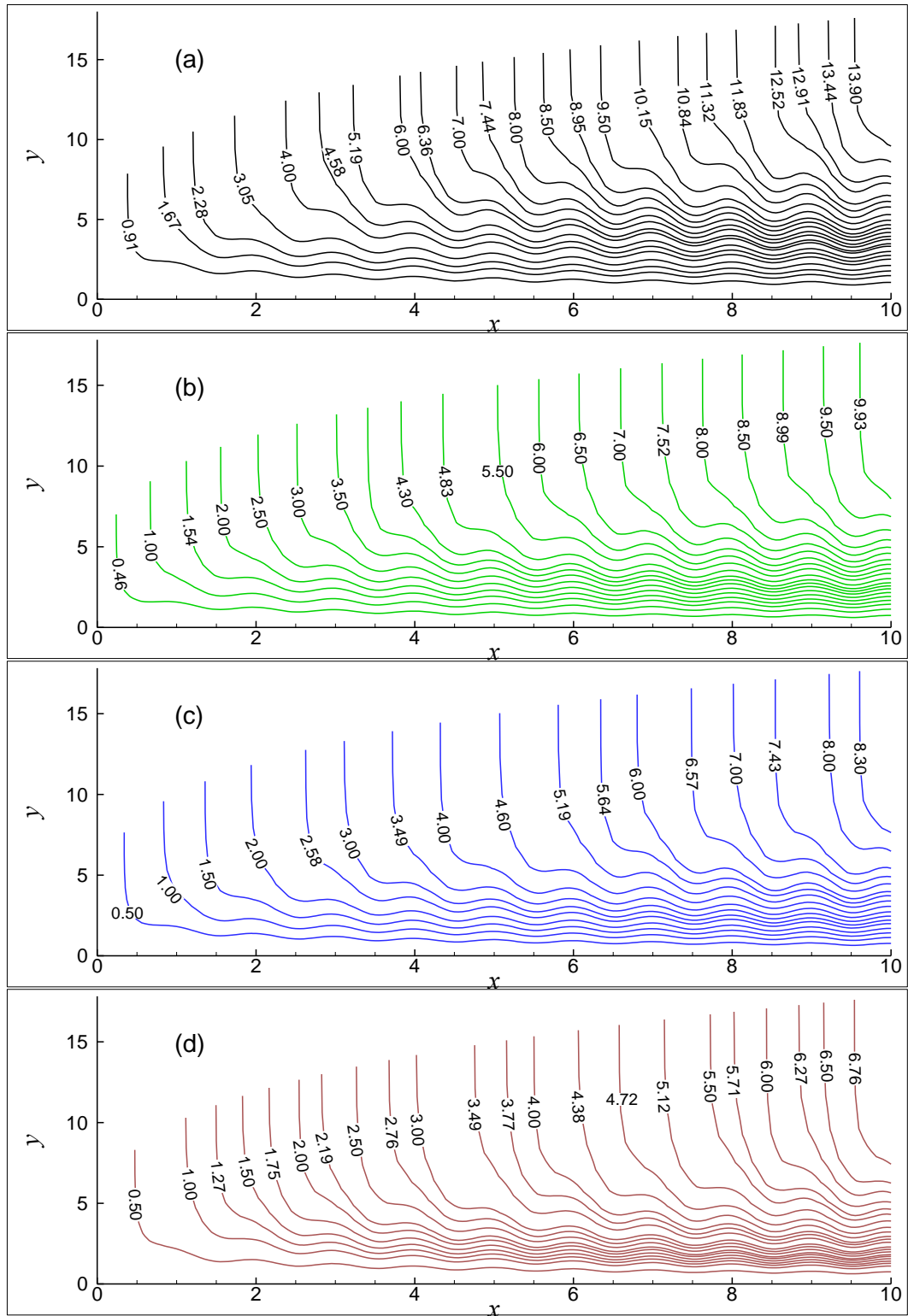


**Figure 3.21:** Streamlines for (a)  $Pr = 0.73$ , (b)  $Pr = 1.74$ , (c)  $Pr = 3.00$  and (d)  $Pr = 7.00$  while  $Q = 0.30$ ,  $\alpha = 0.2$ ,  $J = 0.04$ ,  $Ec = 0.02$ ,  $M = 0.01$

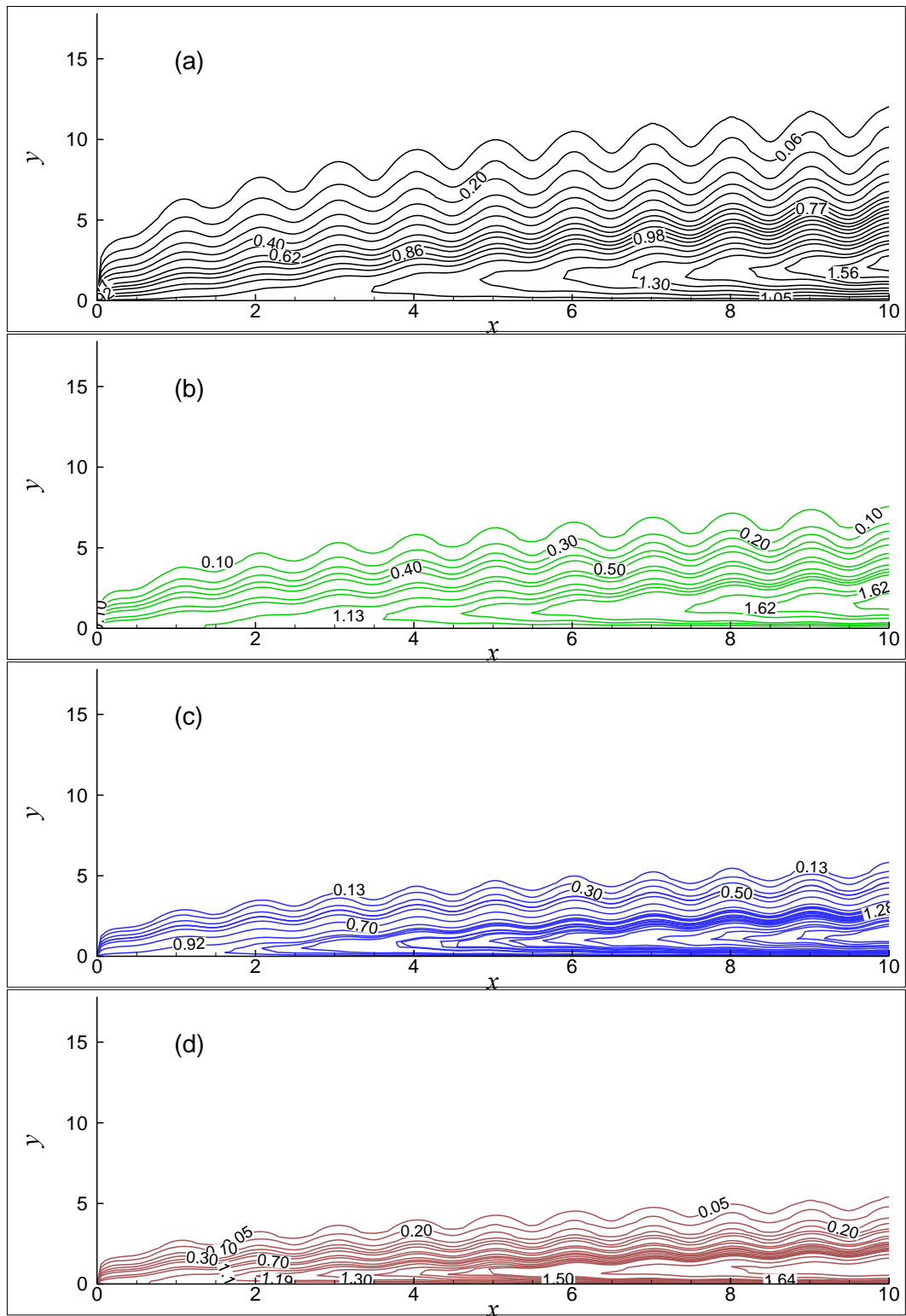


**Figure 3.22:** Isotherms for (a)  $Pr = 0.73$ , (b)  $Pr = 1.74$ , (c)  $Pr = 3.00$  and (d)  $Pr = 7.00$  while  $Q = 0.30$ ,  $\alpha = 0.2$ ,  $J = 0.04$ ,  $Ec = 0.02$ ,  $M = 0.01$

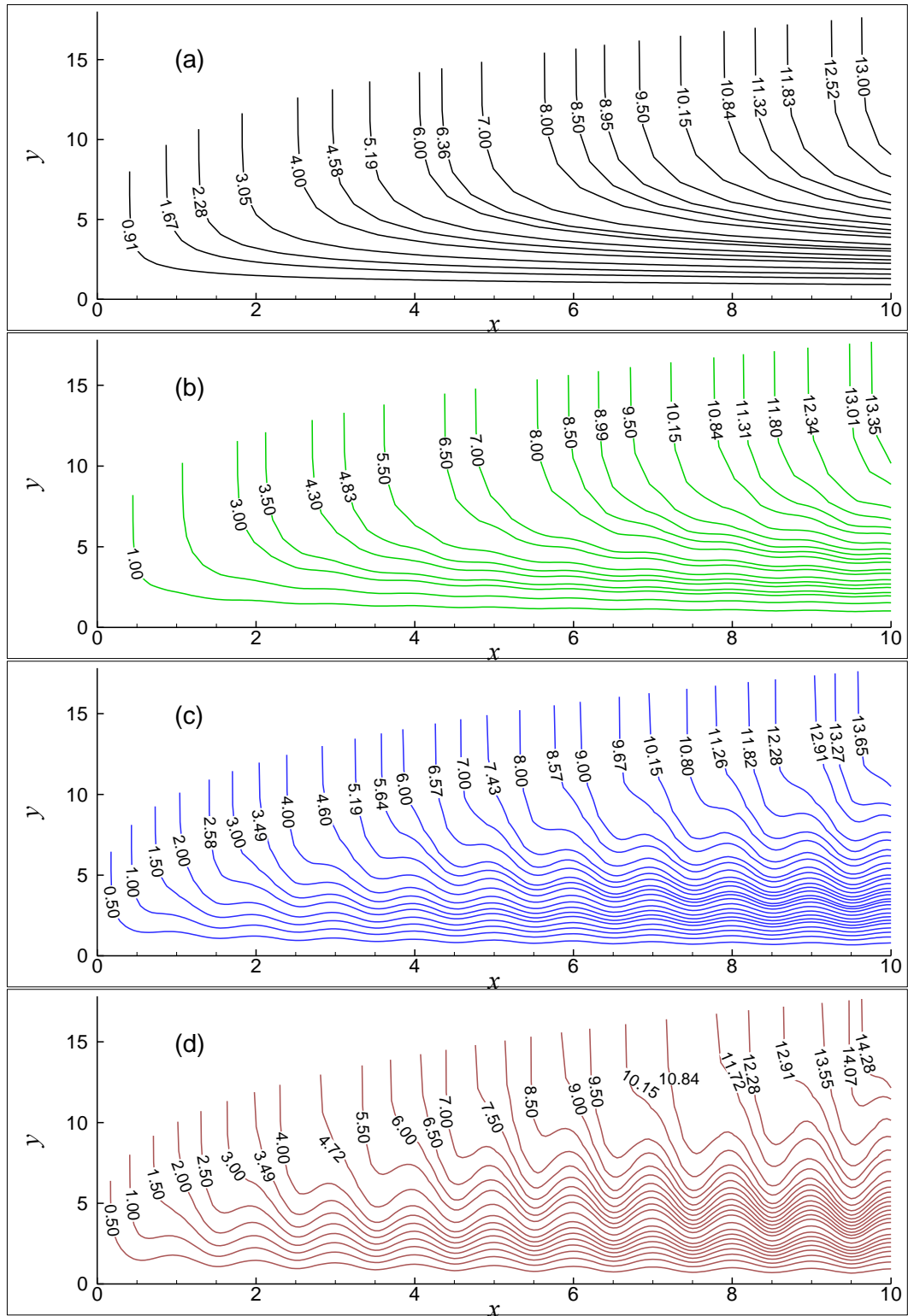


**Figure 3.23:** Streamlines for (a)  $\alpha = 0.0$ , (b)  $\alpha = 0.1$ , (c)  $\alpha = 0.2$  and (d)  $\alpha = 0.3$  while  $Pr = 0.73$ ,  $Q = 0.3$ ,  $J = 0.04$ ,  $Ec = 0.02$ ,  $M = 0.01$

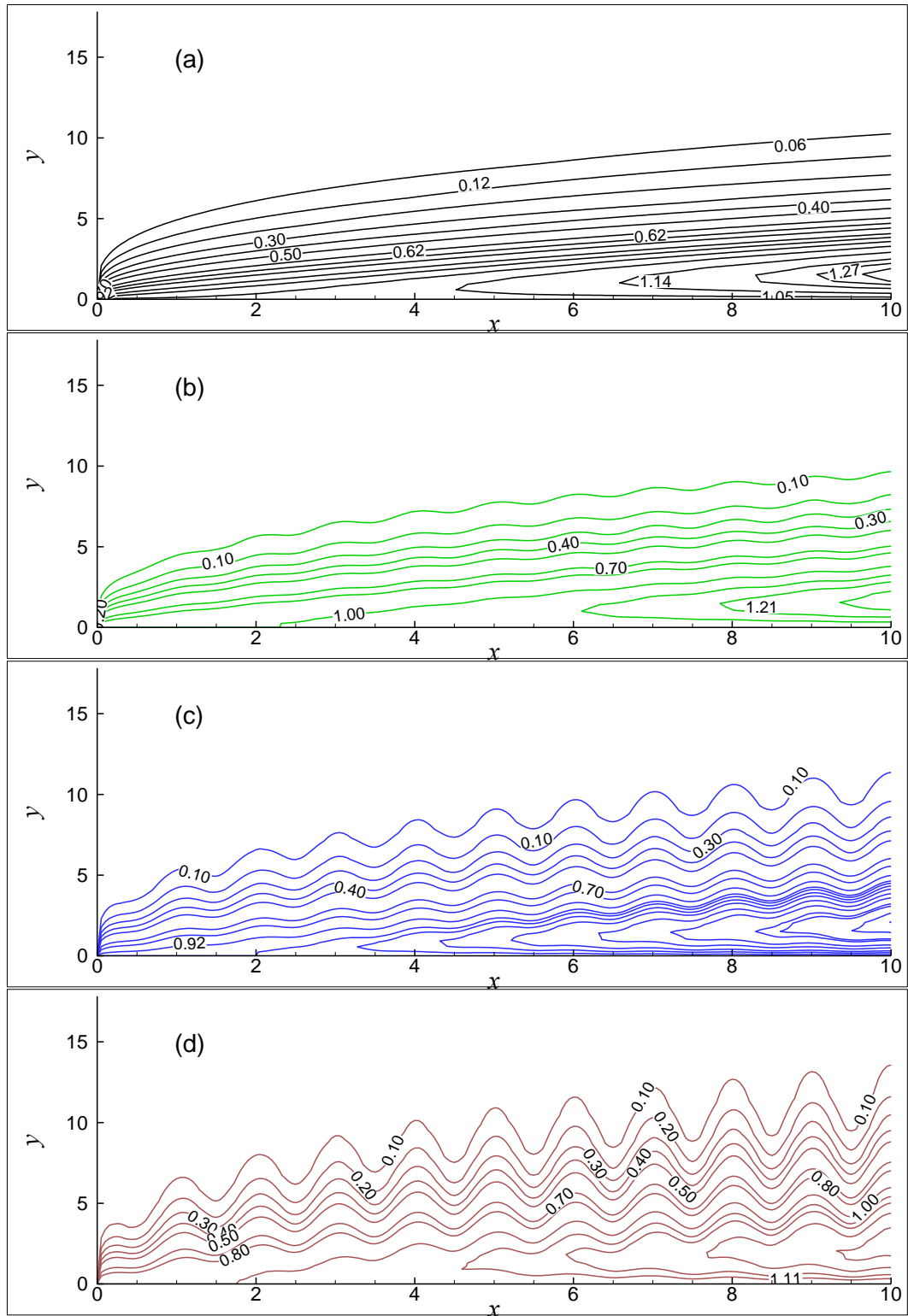


**Figure 3.24:** Isotherms for (a)  $\alpha = 0.0$ , (b)  $\alpha = 0.1$ , (c)  $\alpha = 0.2$  and (d)  $\alpha = 0.3$  while  $Pr = 0.73$ ,  $Q = 0.3$ ,  $J = 0.04$ ,  $Ec = 0.02$ ,  $M = 0.01$



**Table 3.1** : Skin friction coefficient and rate of heat transfer for the different values of Joule Heating parameter ( $J$ )

$X$	Skin friction coefficient			Rate of heat transfer		
	$J = 0.001$	$J = 0.020$	$J = 0.040$	$J = 0.001$	$J = 0.020$	$J = 0.040$
0	0.74227	0.74227	0.74227	.32999	.32999	.32999
1	0.81587	0.81703	0.81824	.09923	.09627	.09314
2	0.86150	0.86506	0.86882	-.01887	-.02874	-.03924
3	0.89715	0.90409	0.91144	-.12056	-.14086	-.16263
4	0.92862	0.93985	0.95179	-.21447	-.24877	-.28587
5	0.95762	0.97401	0.99149	-.30418	-.35618	-.41295
6	0.98496	1.00735	1.03131	-.39142	-.46496	-.54604
7	1.01112	1.04034	1.07169	-.47720	-.57631	-.68666
8	1.03640	1.07325	1.11290	-.56217	-.69107	-.83601
9	1.06098	1.10626	1.15511	-.64680	-.80986	-.99508
10	1.08501	1.13951	1.19846	-.73139	-.93323	-1.16477

Since the figures 3.2 (a) and 3.2 (b) of effects of Joule heating can be seen a little differences, here this table will help us to understand the changes of skin friction coefficient and rate of heat transfer with the changes of Joule heating parameter  $J$ . From the table it is noticed that increasing value of  $J$  increases skin friction and decrease rate of heat transfer.

## Conclusion of this Chapter

The effects of the heat generation parameter  $Q$ , the magnetic parameter  $M$ , the viscous dissipation parameter  $Ec$ , Joule heating parameter  $J$ , the Prandtl number  $Pr$  and the amplitude of the wavy surface  $\alpha$  on natural convection flow of viscous incompressible fluid along a vertical wavy surface have been investigated. From the present investigation the following conclusions may be drawn:

- ❑ The velocity within the boundary layer expands for increasing values of the heat generation parameter, the viscous dissipation parameter, Joule heating parameter and the amplitude-to-length ratio of the wavy surface. On the other hand, the velocity decreases for increasing values of magnetic parameter and the Prandtl number.
- ❑ The temperature within the boundary layer increases for increasing values of the heat generation parameter, the magnetic parameter, the viscous dissipation parameter, Joule heating parameter and the amplitude-to-length ratio of the wavy surface.
- ❑ Increased values of the heat generation parameter, Joule heating parameter and viscous dissipation parameter lead to increase in the skin friction coefficient while the reverse phenomena occurs for increasing values of the magnetic parameter, the Prandtl number and the amplitude-to-length ratio of the wavy surface.
- ❑ The rate of heat transfer decreases with the increase of the heat generation parameter, the magnetic parameter, the viscous dissipation parameter and the amplitude-to-length ratio of the wavy surface but for increasing values of Prandtl number, the rate of heat transfer increase gradually.
- ❑ The increasing velocity enhances velocity boundary layer thickness for the higher values of the heat generation parameter, the viscous dissipation parameter, the amplitude-to-length ratio of the wavy surface. But opposite result is observed for increasing values of the magnetic parameter and the Prandtl number.

- An increase of the values of heat generation parameter, the magnetic parameter, the viscous dissipation parameter and the amplitude-to-length ratio of the wavy surface lead the thermal boundary thicker gradually. But opposite result is observed for increasing values of the Prandtl number  $Pr$ .

### Comparison and code validations

**Table 3.2:** Comparison of the present numerical results of skin friction coefficient,  $f''(x,0)$  and the heat transfer,  $-\theta'(x,0)$  with Hossain et al. (2002) for the variation of Prandtl number  $Pr$  while  $Ec = 0.0$ ,  $M = 0.0$ ,  $J = 0.0$ ,  $Q = 0.0$  with  $\alpha = 0.1$ .

$Pr$	$f''(x,0)$		$\theta'(x,0)$	
	Hossain et al. (2002)	Present work	Hossain et al. (2002)	Present work
1.0	0.908	0.911	0.401	0.400
10.0	0.591	0.593	0.825	0.823
25.0	0.485	0.489	1.066	1.064

Here the magnetic parameter  $M$ , Viscous dissipation parameter  $Ec$ , Joule heating parameter  $J$ , Heat generation parameter  $Q$  are ignored while different values of Prandtl number  $Pr = (1.0, 10.0, 25.0)$  are chosen. From Table 3.2, it is clearly seen that the present results are excellent agreement with the solution of Hossain et Al. (2002)

# Conclusion

---

The present work performs the viscous dissipation effect in presence of heat generation and Joule heating on natural convection flow along a vertical wavy surface. The governing boundary layer equations are first transformed into a non-dimensional form using the appropriate transformations. The resulting nonlinear system of partial differential equations are mapped into the domain of a vertical flat plate and then solved numerically employing the implicit finite difference method, known as Keller-box scheme. Major findings can be summarized as per the following conclusions

## Summary of the major outcomes

The velocity within the boundary layer increases for increasing values of the heat generation parameter  $Q$ , the viscous dissipation parameter  $Ec$  and the amplitude-to-length ratio of the wavy surface  $\alpha$ . Increasing velocity increases the skin friction coefficient  $C_{fx}$  and the velocity boundary layer thickness.

The temperature within the boundary layer increases for increasing values of the heat generation parameter  $Q$ , the Joule heating parameter  $J$ , the viscous dissipation parameter  $Ec$  and the amplitude-to-length ratio of the wavy surface  $\alpha$ . For increasing fluid temperature, the temperature difference between fluid and surface decreases and the correspond rate of heat transfer decreases. It is also observed that the thermal state of the fluid increases, so the thermal boundary layer becomes thicker.

Conclusion

## **Extension of this work**

The present work can be extended in different ways. Some of these are:

- The thermal conductivity as a function of temperature can be considered to extend the present work.
- Complex wavy surface can be considered as a combination of two sinusoidal functions.
- The problem can be extended considering the radiation effect.
- Forced convection may be studied with the same geometry.
- Mixed convection may be studied with the same geometry.

## References

Anjali Devi S.P. and Kayalvizhi M., (2010): Viscous dissipation and radiation effects on the thermal boundary layer flow with heat and mass transfer over a non-isothermal stretching sheet with internal heat generation embedded in a porous medium, *Int. J. Energy Technology*, Vol. 2(20), pp. 1-10.

Alam M.M., Alim M.A. and Chowdhury M.M.K., (2007): Viscous dissipation effects on mhd natural convection flow over a sphere in the presence of heat generation, *Nonlinear Analysis: Modelling and Control*, Vol. 12, No.4, 447-459.

Azim M., Mamun A. and Rahman M., (2010): Viscous Joule heating MHD conjugate heat transfer for a vertical flat plate in the presence of heat generation, *International Communications in Heat and Mass Transfer*, Vol.37, no. 6, pp. 666-674.

Bhavnani S.H. and Bergles A. E., (1991): Natural convection heat transfer from sinusoidal wavy surface, *Waerme-Stoffuebertrag.*, Vol.26, pp. 341-349.

Cebeci T. and Bradshaw P., (1984): *Physical and computational aspects of convective heat transfer*, Springer, New York.

Chamkha A.J., (2002): Effects of magnetic field and heat generation/absorption on natural convection from an isothermal surface in a stratified environment, *International Journal of Fluid Mechanics Research*, Vol. 29, pp. 669-681.

Chamkha A.J., Al-Mudhaf A. and Pop I., (2006): Effect of heat generation or absorption on thermophoretic free convection boundary layer from a vertical flat plate embedded in a porous medium, *International Communications in Heat and Mass Transfer*, Vol. 33, pp. 1096-1102.

Chamkha A.J. and Aly A.M., (2011): MHD free convection flow of a nanofluid past a vertical plate in the presence of heat generation or absorption effects, *Chemical Engineering Communications*, Vol. 198, pp. 425-441.

Gebhart B., (1962): Effects of viscous dissipation in natural convection, *J. Fluid Mech.*, Vol. 14, pp. 225-232.

Gebhart B. and Mollendorf J., (1969): Viscous dissipation in external natural convection flows, *J. Fluid Mech.*, Vol. 38, No. 1, pp. 97-107.

Hossain M.A., Kabir S. and Rees, D.A.S., (2002): Natural convection of fluid with variable viscosity from a heated vertical wavy surface, *Z. Angew. Math. Phys.*, Vol. 53, pp. 48-52.

Hossain M.A. and Rees D.A.S., (1999): Combined heat and mass transfer in natural convection flow from a vertical wavy surface, *Acta Mechanica*, Vol. 136, pp. 133-141

## References

Jang J.H., Yan W.M. and Liu H.C.,(2003): Natural convection heat and mass transfer along a vertical wavy surface, *Int. J. Heat Mass Transfer*, Vol. 46, pp. 1075-1083.

Jha B.K. and Ajibade A.O., (2011): Effect of viscous dissipation on natural convection flow between vertical parallel plates with time-periodic boundary conditions, *J. Thermophysics and Aeromechanics*, Vol. 18, Issue 4, pp 561-571.

Keller H.B., (1978): Numerical methods in boundary layer theory, *Ann. Rev. Fluid Mech.*, Vol. 10, pp. 417-433.

Kim E., (1997): Natural convection along a wavy vertical plate to non-newtonian fluids, *Int. J. Heat Mass Transfer*, Vol.40, pp. 3069-3078.

Moulic S,G. and Yao L.S., (1989): Natural convection along a wavy surface with uniform heat flux, *ASME J. Heat Transfer*, Vol. 111, pp. 1106-1108.

Molla M.M., Hossain M.A. and Yao L.S., (2004): Natural convection flow along a vertical wavy surface with uniform surface temperature in presence of heat generation/absorption, *Int. J. Therm. Sci.*, Vol. 43, pp. 157-163.

Mamun A.A., Chowdhury Z.R., Azim M.A. and Molla M. M., (2008): MHD-conjugate heat transfer analysis for a vertical flat plate in presence of viscous dissipation and heat generation, *Int. comm. Heat Transfer*, Vol. 35, pp. 1275-1280.

Molla M.M. and Hossain M.A., (2007): Radiation effect on mixed convection laminar flow along a vertical wavy surface, *Int. J. Thermal Sciences*, Vol. 46, pp. 926-935.

Palani G and Kim K.Y., (2011): Joule heating and viscous dissipation effects on MHD flow past a semi-infinite inclined plate with variable surface temperature, *J.Engineering Thermophysics*, Vol. 20, Issue 4, pp 501-517.

Parveen N. and Alim M.A., (2011): Effect of temperature-dependent variable viscosity on magnetohydrodynamic natural convection flow along a vertical wavy surface, *International Scholarly Research Network Mechanical Engineering*, Vol.2011, Article ID 505673, pp. 1-10.

Parveen N. and Alim M.A., (2012): MHD free convection flow along a vertical wavy surface with temperature dependent thermal conductivity in presence of heat generation, *Int. J. Energy Technology*, Vol.4, pp.1-9.

Parveen N. and Alim M.A., (2013): Joule heating and MHD free convection flow along a vertical wavy surface with viscosity and thermal conductivity dependent on temperature, *J. Naval Architecture and Marine Engineering*, Vol. 10 (2), pp. 81-98.

Parveen N. and Alim M.A., (2014): Numerical solution of temperature dependent thermal conductivity on MHD free convection flow with joule heating along a vertical wavy surface. *Journal of Mechanical Engineering*, Vol.ME 44, No.1, pp.43-50.

## References

Vejravelu K and Hadjinicolaou A., (1993): Heat transfer in a viscous fluid over a stretching sheet with viscous dissipation and internal heat generation, *Int. comm. Heat Transfer*, Vol. 20, pp. 417-430.

Wang C.C. and Chen C.K., (2001): Transient forced and free convection along a vertical wavy surface in micropolar fluid, *Int. J. Heat Mass Transfer*, Vol. 44, pp. 3241-3251.

Yao L.S., (1983): Natural convection along a vertical wavy surface, *ASME J. Heat Transfer*, Vol. 105, pp. 465-468.